Defense Nuclear Agency
6801 Telegraph Road
Alexandria, Virginia 22310-3398

OPSSI

1 March 1996

MEMORANDUM FOR DISTRIBUTION

SUBJECT: Declassification Review of Operation TEAPOT Test Reports

The following 106 reports concerning the atmospheric nuclear tests conducted during Operation TEAPOT in 1955 have been declassified and cleared for open publication/public release:

WT-1101 thru WT-1114, WT-1117, WT-1119, WT-1120, WT-1122 thru WT-1152, WT-1154 thru WT-1156, WT-1158, WT-1161 thru WT-1166, WT-1168 thru WT-1178, WT-1178A, WT-1179 thru WT-1199, WT-1209, WT-1212 thru WT-1218, WT-1220, WT-1222, WT-1225, WT-1226, and WT-1228 thru WT-1230

An additional 8 WTs from TEAPOT have been re-issued with deletions and are identified with an "EX" after the WT number. These reissued versions are unclassified and approved for open publication. They are:

WT-1115, WT-1116, WT-1118, WT-1121, WT-1153, WT-1204, WT-1206, and WT-1208

This memorandum supersedes the Defense Nuclear Agency, ISTS memorandum same subject dated August 17, 1995 and may be cited as the authority to declassify copies of any of the reports listed in the first paragraph above.

for RITA M. METRO
Chief, Information Security Section

Operation TEAPOT

NEVADA TEST SITE

February – May 1955

Project 2.6

RADIATION ENERGY ABSORBED BY HUMAN PHANTOMS IN A FISSION FALLOUT FIELD

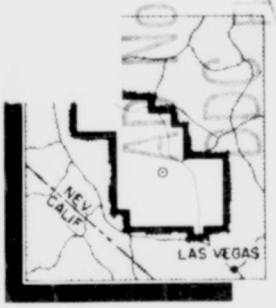

RESTRICTED DATA

This document contains restricted data as defined in the Atomic Energy Act of 1954. Its transmittal or the disclosure of its contents in any manner to an unauthorized person is prohibited.

HEADQUARTERS FIELD COMMAND, ARMED FORCES SPECIAL WEAPONS PROJECT
SANDIA BASE, ALBUQUERQUE, NEW MEXICO

[redacted]

WT-1120

This document consists of 60 pages

No. 175 of 265 copies, Series A

OPERATION TEAPOT

Project 2.6

RADIATION ENERGY ABSORBED BY HUMAN PHANTOMS IN A FISSION FALLOUT FIELD

by

George W. Imirie, Jr.

and

Robert Sharp

RESTRICTED DATA

This document contains restricted data as defined in the Atomic Energy Act of 1954. Its transmittal or the disclosure of its contents in any manner to an unauthorized person is prohibited.

U. S. NAVAL MEDICAL RESEARCH INSTITUTE
BETHESDA, MARYLAND

[redacted]

SUMMARY SHOT DATA

SHOT	CODE NAME	DATE	TIME *	AREA	TYPE	LATITUDE & LONGITUDE OF GROUND ZERO
1	Wasp	18 February	1200	T-7-4 1/	762' Air	37° 05' 11.6856" 116° 01' 18.7366"
2	Moth	22 February	0545	T-3	300' Tower	37° 02' 52.2654" 116° 01' 15.6967"
3	Tesla	1 March	0530	T-9b	300' Tower	37° 07' 31.5737" 116° 02' 51.0077"
4	Turk	7 March	0520	T-2	500' Tower	37° 08' 18.4944" 116° 07' 03.1679"
5	Hornet	12 March	0520	T-3a	300' Tower	37° 02' 25.4043" 116° 01' 31.3674"
6	Bee	22 March	0505	T-7-1a	500' Tower	37° 05' 41.3880" 116° 01' 25.5474"
7	ESS	23 March	1230	T-10a	67' Underground	37° 10' 06.1263" 116° 02' 37.7010"
8	Apple	29 March	0455	T-4	500' Tower	37° 05' 43.9200" 116° 06' 09.9040"
9	Wasp'	29 March	1000	T-7-4 2/	740' Air	37° 05' 11.6856" 116° 01' 18.7366"
10	HA	6 April	1000	T-5 3/	36620' MSL Air	37° 01' 43.3642" 116° 03' 28.2624"
11	Post	9 April	0430	T-9c	300' Tower	37° 07' 19.6965" 116° 02' 03.8860"
12	MET	15 April	1115	FF	400' Tower	36° 47' 52.6887" 115° 55' 44.1086"
13	Apple 2	5 May	0510	T-1	500' Tower	36° 03' 11.1095" 116° 06' 09.4937"
14	Zucchini	15 May	0500	T-7-1a	500' Tower	37° 05' 41.3880" 116° 01' 25.5474"

* APPROXIMATE LOCAL TIME - PST PRIOR TO 24 APRIL, PDT AFTER 24 APRIL
1/ ACTUAL GROUND ZERO 36' NORTH, 426' WEST OF T-7-4
2/ ACTUAL GROUND ZERO 94' NORTH, 62' WEST OF T-7-4
3/ ACTUAL GROUND ZERO 36' SOUTH, 397' WEST OF T-5

ABSTRACT

Actual methods used to evaluate total radiation doses received by personnel operating in residual fallout fields are questionable, due to the limitations of present radiac monitoring equipment. The military, in order to plan better operations in nuclear warfare, must have accurate knowledge of the hazards to be encountered. The planned objectives are aimed at evaluating the total energy absorbed; pointing out the inadequacies of present field instruments and the existence of an additional hazard to personnel.

Phantoms, resembling humans and made of tissue equivalent materials, were placed in prone and upright positions in a fallout field. Measurements of dose received were taken over the surface and at several internal locations corresponding to the positions of vital organs.

The presence of a soft component, strongly indicative of beta radiation, was found which gave a surface dose, in many cases, 50 times the average internal dose for a man lying prone. This factor can be reduced approximately 50 percent by brushing the ground, but this apparently has little effect on the internal dose. The upright man in such a field received doses differing by a factor of eight between feet and head. Although the internal doses agreed favorably with standard radiac equipment, the surface dose was found to be significantly greater.

It is concluded that a fallout field delivers a large dose of absorbed energy to the body, which is not usually measured. Further study is required to determine the biological hazard of the unmeasured components.

FOREWORD

This is one of the reports presenting the results of the 47 projects participating in the Military Effects Tests Program of Operation TEAPOT, which included 14 test detonations. For readers interested in other pertinent test information, reference is made to WT-1153, Summary Report of the Technical Director, Military Effects Program. This summary report includes the following information of possible general interest:

a. An over-all description of each detonation, including yield, height of burst, ground zero location, time of detonation, ambient atmospheric conditions at detonation, etc., for the 14 shots.

b. Discussion of all project results.

c. A summary of each project, including objectives and results.

d. A complete listing of all reports covering the Military Effects Tests Program.

ACKNOWLEDGMENTS

The authors wish to acknowledge the efforts of those six men who actually participated in the field work: A. R. Holtry, G. C. Weiss, G. I. Jameson, C. R. Biles, J. W. Duckworth, J. T. Istock.

In addition, the expert advice of the following is acknowledged: G. Failla, K. Z. Morgan, H. I. Roth, J. E. Morgan.

CONTENTS

TABLES

CHAPTER I

INTRODUCTION

1.1 OBJECTIVES

The objectives of Project 2.6, Operation TEAPOT, were to (1) measure surface dosage and depth dosage in unit density simulated-human phantoms, in order to estimate the relative contributions of beta and gamma radiation to the total surface dose, and obtain the total dose received at the locations of the various vital organs of the human body; (2) aid in the interpretation of the physical characteristics of the residual fields encountered; and (3) compare the estimate of radiological hazard, as indicated by the results of this experiment, with the estimate of radiological hazard, as indicated by existing radiological survey techniques and hazard criteria.

All these measurements were coordinated to several variables: vertical gradation of dose, change of character of radiation with time and distance from ground zero, and changes in the beta to gamma ratio.

Accurate knowledge of both the quantity and quality of radiation is essential to effective personnel dosimetry and to the prognosis of calculated risk exposures, which may under certain conditions become predictable. A proper estimate of the total radiation hazard may revise some present estimates of human tolerance and may also have a bearing on the future design of certain dosimetric instruments.

1.2 BACKGROUND

In any consideration of the problems of radiological defense, the personnel hazard of a fallout field deserves a position of prime importance. The work reported herein is considered a realistic approach to the evaluation of the relative hazards of the various nuclear radiations present in such a field. It is well known that both gamma radiation and beta particles are emitted by radionuclides formed in a nuclear detonation. Hence, anywhere within the air range of the most energetic beta radiation present the possibility that a hazard exists must be considered.

Considerably less attention has been paid to beta particle exposure in comparison to gamma ray exposure. It has been assumed in the past, to a great extent, that exposure to beta radiation is relatively non-injurious unless the dose received is unusually large. This assumption probably has been based on consideration of the relative non-penetrating power of beta particles and the shielding afforded by the normal covering of clothes. Condit, Dyson, and Lamb (1) questioned the validity of these assumptions on the basis of theoretical calculations.

Reference 1 based its conclusion (that a significant beta hazard exists) on the assumption that: (1) the contaminated area must be considered an infinite plane surface only, so that self-absorption is negligible; (2) the average energy of all beta particles emitted is 1 Mev; (3) fission products produce two beta particles per gamma photon; and (4) fission beta particles are almost completely absorbed in transversing 2 meters of air, which absorbs a negligible quantity of gamma radiation.

Parker's (2) data shows that the ionization per unit path length of a beta particle is approximately 75 times greater than a gamma of similar energy. Adding this to the aforementioned points, a beta dose rate at any surface point is derived which is 150 times that of a gamma ray dose rate from a point source of fission products.

1.2.1 Reduction of Beta Hazard. Brennan (3) has discussed six factors which tend to reduce the possible beta hazard: (1) The normal clothing of a person may provide some shielding from beta radiation with the degree of shielding directly dependent on the energy of the beta radiation; (2) The small percentage of bremsstrahlung produced by high energy beta radiation will be measured by most personnel-monitoring instruments; (3) The cornified layer of human tissue, approximately 7 mg/cm^2 thick, does present an effective barrier for betas of less than 0.1 Mev energy; (4) The idealized plane of uniformly spread fission products does not actually exist in the field; (5) The accepted permissible dose for localized beta radiation is larger than the permissible whole body gamma dose; and (6) Beta radiation (unlike gamma radiation) presents a possible hazard, in a fallout field, only to the body surface facing the beta emitting fission products.

Further consideration of these factors are necessary in order to bring beta hazard into proper prospective. Unfortunately, clothing may increase rather than decrease the beta hazard, since it is likely that clothing may collect contaminated dust or dirt and localize it near the skin, thus becoming a contact source. Since bremsstrahlung is only produced by high energy beta radiation, and then only to a small percent, it is not a suitable index of quantitative detection for the lower beta ray energies (0.5-1.0 Mev) which still possess body damaging power.

The tiny crevices of the cornified layer of human skin provide an ideal depository for the collection of contaminated dirt. This condition provides the situation where it would be possible to suffer an incapacitating localized beta burn while receiving a relatively low whole body gamma dose. This phenomenon was observed on the Marshallese natives (4).

The actual radiation hazard, resulting from the unmeasured beta radiation by most detection instruments, is not as large a factor as might be supposed by theoretical calculation, but is a factor of 30:1 or less. However, Brennan states that his surface measurements were made above a manikin's surface which led to low surface-to-vital organ dose ratios because the geometry does not provide for saturation back-scatter.

The scattering of beta radiation is one of the principal reasons why a surface dose is much larger from a source of beta radiation than that from a gamma source. Although the ionization along the irregular track of the beta particle is much greater than that produced along the forward track of the photon, it is this irregularity of the beta particle track which causes it to deliver its dose much closer to the surface.

1.2.2 Previous Work by Others. Dahl (5), although engaged only in the assay of residual gamma radiation, found results that he believed could be most plausibly explained by the presence of large amounts of beta radiation. He would not eliminate the possibility of the presence of low energy gamma rays (5 to 15 kev) but he suggests that their presence is unlikely.

Much evidence has been cited to support the conclusion that the use of unit density material for the determination of effective gamma ray energy by depth dose curves is impossible. This is due to the actual energy absorbed per unit mass being nearly constant over a wide range (60 to 2000 kev) of gamma ray energies (5).

This project, although in agreement with this, have included a depth dose determination in phantoms for the purpose of predicting dose-at-a-depth based on surface dose readings. Thus, this project is concerned with total radiation dose rather than effective energy of that radiation.

Tochilin (6) has provided much physical data regarding both beta and gamma radiation in a fallout field. These results indicate a beta energy of 1.7 Mev max., an effective gamma energy of approximately 130 kev, and a beta-to-gamma ratio of 19:1. These values were stated to be estimates, because the wave length response of the film detectors was such that the specific density of the film per roentgen-equivalent-physical was unknown, unless the spectrum of the radiation was known. It will be shown later in this report that the use of such physical data in the interpretation of biological dose is difficult.

CHAPTER 2

THEORY

2.1 PURPOSE OF HUMAN PHANTOMS

Generally, the quantity and quality of a source of radiation can be determined by many known methods of evaluation in use today. With knowledge of the scatter cross-sections and attenuation coefficients of several different materials, it is theoretically possible to calculate these values for tissue, hence providing a means for calculating the tissue dose. The application of this procedure becomes prohibitively difficult when the multidirectionality of radiation, the complex beta and gamma ray spectrums, and the geometry presented by a human being in a fallout field are considered.

Therefore, the ultimate answer to the evaluation of tissue dose is to use a human body well instrumented with finite size detectors, which in themselves are also composed of tissue in order not to introduce into the absorbing system any foreign material. Since this is neither possible nor practical to date, a substitute method must be found; this is the purpose of the human phantoms used in this work. These phantoms, in order to closely approximate the ultimate aim, must be fabricated of tissue-equivalent material in the detailed shape of a human and must be well instrumented with small, low atomic number detectors.

2.2 DETECTORS

The detector should be composed of material of essentially the same effective Z-number as tissue and be physically small, in order not to disturb the geometry of the human body any more than necessary.

All normally available radiation detectors were eliminated for use by Project 2.6, primarily because: (1) the physical size of almost every common detector is prohibitive since it would destroy the geometry of the human phantom; (2) the high Z materials used in the construction of most instruments will set up scattering processes unlike those of tissue; (3) most detector walls are too thick to provide entrance to beta radiation; and (4) the gamma wave length response of most detectors is undesirable.

Project 2.6 has attempted to construct and use a detector which substantially overcomes these four objections to available detectors.

2.3 ABSORBED VERSUS DELIVERED DOSE

A hazard may exist at any time tissue is exposed to electromagnetic or corpuscular radiation, because of energy absorbed within the tissue due to the ionization produced by the interaction of these radiations with the tissue. The concepts of "energy absorbed" and "ionization produced per unit volume" have been treated synonymously. In actuality, since one is the cause of the other, the proper evaluation of tissue damage can best be expressed in terms of energy absorbed. The precise biological significance of energy absorbed is not entirely clear. Whereas a large portion of the incident energy may be utilized in the production of ions in the medium, there is an appreciable fraction of the absorbed energy utilized by processes in which no ions are formed; e.g., excitation of atoms and decomposition of complex molecules. Although energy absorbed and ionization produced per unit volume are absolute measures of tissue dose (true only within the definition limits of several dose units) there still remain important uncertainties in the actual measurement of ionization and in both the physical and biological significance of energy absorbed.

The roentgen, by its definition, is only a partial description of the electromagnetic radiation at a point measured in terms of ionization produced in air. The relationship that does exist between the energy absorbed in air corresponding to 1 r and energy flux demonstrates a complicated dependence upon photon wave length. The roentgen, which is only applicable to X or gamma radiation, is only a partial description of the radiation at any specified point. This point need not necessarily be within the absorbing medium itself. The roentgen, by definition, refers to ion pair production (and consequent energy absorption) in air; however, a material of high Z and high density will absorb more energy for the same flux of radiation that produces the 83 ergs/gm of air which constitutes a dose of 1 r. Therefore, a dose expressed in roentgens is dependent on the absorbing medium and, hence, the amount of energy that particular medium absorbs.

Many units of dose have been proposed to circumvent the limitations of the roentgen; e.g., rep, rem, gram-roentgen, etc. These units, although enjoying widespread usage, have not been accepted by international agreement; the roentgen has. The International Commission on Radiological Units recommended that a distinction be made between dose in the general sense and absorbed dose, the unit recommended being the rad. The rad is defined as an absorbed dose of 100 ergs/gm imparted to any matter by an ionizing radiation at the point of interest.

Inasmuch as the fission fallout field has present both electromagnetic and corpuscular radiations and a wide variety of spectral complexities of each, it is logical to evaluate total human dose in terms of energy absorbed. Since modern day standards of instrumentation are based upon measurements utilizing the roentgen, an evaluation of a tissue equivalent reading device is not possible. An ionization detecting device composed of tissue equivalent materials within a

tissue medium would afford the closest approximation to recording a true tissue dose. This is the approach followed by Project 2.6.

2.4 RADIATION MEASUREMENT PROBLEMS

Most radiation survey meters, often beta detecting, are wave length independent to gamma radiation only above 80 kev. The reasons underlying the selection of 80 kev as the lower limit criteria, or specification, of satisfactory instrumentation is not apparent to Project 2.6. Much work is now in progress attempting to evaluate the biological hazard of gamma energies lower than 80 kev. Until the results of this work demonstrate a relative insignificance of hazard from this low energy radiation spectrum, it would be more scientific to assume the existence of a hazard rather than to subrogate it to unimportance. In consideration of the high specific ionization of this energy gamma radiation, it would appear speculative as to whether the unimportance of this radiation to biological hazard can be substantiated. Therefore, it is highly desirable to lower the 80-kev cutoff of wavelength independence in so far as possible to better evaluate human radiation dosages.

Because of the corpuscular nature of beta radiation, proper dosage measurements are sufficiently difficult to the extent that they are often by-passed.

Radiation survey equipment generally is limited for two reasons: (1) the manner of absorption of beta radiation eliminates the extrapolation of a dosage reading for a point of interest from a reading taken at some other reference point; and (2) the design of a single unit to properly record dose from all energies of gamma radiation is practically impossible.

In view of the choice of a poor unit of dose (the roentgen), the gamma wave length dependence of most detectors, and the difficult task of measuring beta radiation, it appears that present day human hazard instrumentation is in need of much revision. Because of the relative biological effectiveness of beta and gamma radiation, not to mention the effects of different energies of each, a cooperative consolidated effort on the part of both the physicist and the biologist is indicated to resolve these difficulties.

CHAPTER 3

INSTRUMENTATION

Each phase of the instrumentation used in the collection of data will be described separately. The manner in which this equipment was used will be explained in Chapter 4.

3.1 FIELD UNITS

The experimental design for this project involved the use of simulated human phantoms made completely of laminated, pressed wood (density approximately 1.08). These phantoms were constructed to conform rather closely to average man dimensions and featured a hollowed chest cavity filled with plastic sponge to simulate lung material and a flat-front side from sternum to ankle. The latter feature made it possible to place the phantom on short pegs in a prone position and maintain the front surface equidistantly parallel 5 cm above the ground. These phantoms were 5-feet, 10-inches tall and weighed 160 pounds each.

Type-A phantom (Figure 3.1) was routed to accommodate a system of pressed wood blocks (Figure 3.2) and plugs (Figure 3.3), which were in turn drilled to accommodate miniature ionization detectors. Each block, when embedded flush in the phantom surface, displayed five detectors for the measurement of surface radiation. Surface blocks were situated in 17 locations over the phantom. Removable pressed wood plugs were used to position additional detectors within the phantom at locations approximating those of the principal vital organs. A removable pressed wood bar (Figure 3.3), drilled to accommodate detectors at several depths through the body, was positioned through the lower abdomen to permit a conventional depth-dose study. This location provided the most uniform scatter environment available and represented an average height with the phantom in an upright position.

The Type-B phantom (Figure 3.4) was designed to obtain basic absorption data using several sets of absorbers (Figure 3.5), each set of a different atomic number. Again the abdominal surface was chosen to provide the most uniform scatter and backing environment. Using a full-scale model phantom provided a realistic, or practical, aspect for any data taken. Removable pressed-wood blocks, each containing five

detectors, were mounted flush with the phantom surface. All were fashioned with uniform area and varied only in thickness. The intended normal position of this phantom was prone on short pegs, with the filter section parallel to the ground.

The final field unit was called the "kite" (Figure 3.6) and consisted of a lightly constructed wooded framework designed to accommodate 43 of the previously described exposure blocks. These blocks were arranged and fitted to provide absorption curves in both tissue equivalent material and gold, each at two heights of approximately 5 cm and 100 cm. Also thin-walled detectors could be exposed at various heights above the ground from 5 cm to 180 cm for the purpose of studying the vertical gradation of air dose.

3.2 IONIZATION CHAMBER

The principle radiation detector used throughout this work consisted of a miniature ionization chamber (Figure 3.7), featuring tissue equivalent material walls (hard gelatin). The removable wall or cap (Figure 3.8) was fashioned in several different thicknesses ranging from 6.35 mg/cm^2 to 13.02 mg/cm^2. When placed in a pressed wood exposure block, which was covered with a 2 mg/cm^2 Saran plastic window, a minimum of 8.35 mg/cm^2 effective wall thickness was realized.

This chamber is a modification of the detectors described by Chambers (7), which were successfully used in several previous field tests. Because of the chamber's small ionizing volume of approximately 0.08 cm^3 and relatively thin chamber-wall construction, a smooth response to beta or very soft gamma radiation was anticipated. A condenser-type construction employing Kel-F insulation and a properly chosen antenna and outer wall diameter provided a detector with excellent stability and good radiation-response characteristics. The sensitivity limits could approach a span of three decades; 0.2 to 200 r. By using five detectors for each experimental point, with agreement quite often within 10 percent, it was surmised that the statistical value of the data obtained would appear adequate.

3.2.1 Beta Response of the Chamber. This chamber was empirically calibrated by using an extrapolation ionization chamber. The chamber is wave length independent of energy in terms of esu/cc corrected for wall absorption.

An inspection of Figure 3.9 shows that this chamber, operated at full saturation voltage, will detect over 70 percent of all beta particles with energies exceeding 0.5 Mev, and 30 percent of those of 0.2 Mev. In as much as the epidermal layer of the standard man is 7 mg/cm^2 thick, it is not reasonable to attach great importance to those beta particles having energies of less than 0.2 Mev, because of their low penetration into the dermis.

3.2.2 Gamma Response of the Chamber. This detector used by itself (i.e., not in a masonite block) is wave length dependent, as shown in Figure 3.10. However, when exposures are made in a masonite block, the wave length response becomes quite good, as shown in Figure 3.11. Actually, it can be shown that the peak of wave length

dependence between 15 and 50 kev is not particularly serious for gamma measurements in a fallout field, since several investigators have shown that there is little gamma radiation within this energy region (6).

The loss in voltage per unit quantity of radiation received by the detector is quite linear, as shown in Figure 3.12.

Dose rates as high as 50 r/min have been applied to these chambers without any breakdown of response. Rarely, in actual practice, would a chamber ever be placed in a field greater than 5 r/min.

3.3 AUTOMATIC READER

Inasmuch as 2,000 miniature ionization chambers were employed in each run, it became imperative to provide an automatic method of recording this data. Since these chambers work on the principle that a loss in original voltage is directly equivalent to a calibrated quantity of radiation, the system of reading steps must be employed either manually or automatically in the following order: (1) read the residual charge left on the detector after exposure to radiation; (2) recharge the chamber to full voltage; (3) read the fully charged chamber; and (4) recharge the chamber to full voltage.

An automatic reader (Figure 3.13) was designed to read 600 chambers/hr and graphically record the data on Esterline-Angus charts. The system is composed of two identical units, each consisting of an electrometer, a precision capacitor, an Esterline-Angus recorder, and a charging supply. These two systems, while working independently of one another, must be perfectly synchronized so that the starting point of the two recorder traces are congruent. That is, the first unit performs Steps 1 and 2, recording the residual charged voltage on the recorder's tape. Four minutes later the second unit performs Steps 3 and 4 and the second recorder must superimpose its trace on the original.

The capacitors used are precision variable air condensers, General Radio, Model 722 DQ, with a range from 25 to 1150 $\mu\mu$f. These capacitors are fixed at 80 $\mu\mu$f for all use. The function of these capacitors is to act as splitting condensers, so that the electrometers read only a particular percentage of the total charge, approximately 5 percent.

The electrometer used was a Keithly Model 210 with a variable range of 0.8, 2.0, 8.0, 20.0, and 80.0 volt. This electrometer was specifically selected for several reasons: its good stability, high sensitivity, ac-operation, and physical construction.

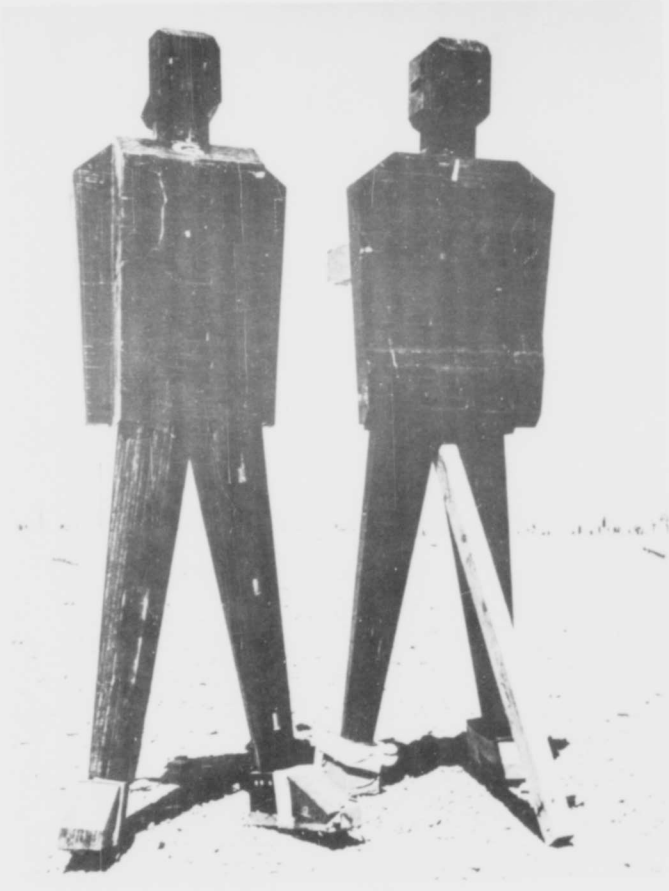

Figure 3.1 Type-A simulated human phantom.

Figure 3.2 Pressed wood surface blocks.

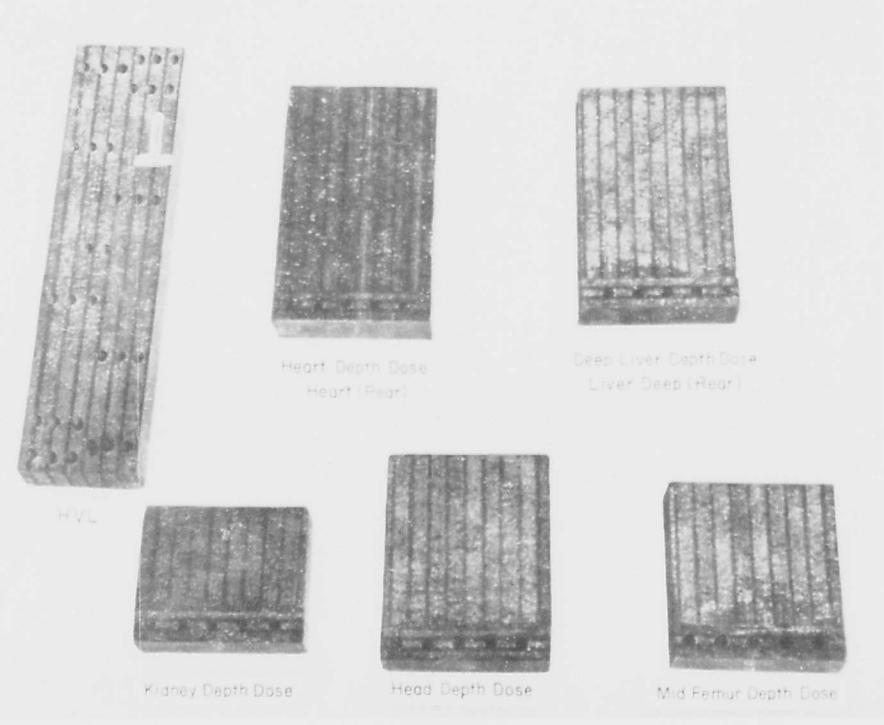

Figure 3.3 Pressed wood depth plugs and half-value layer bar.

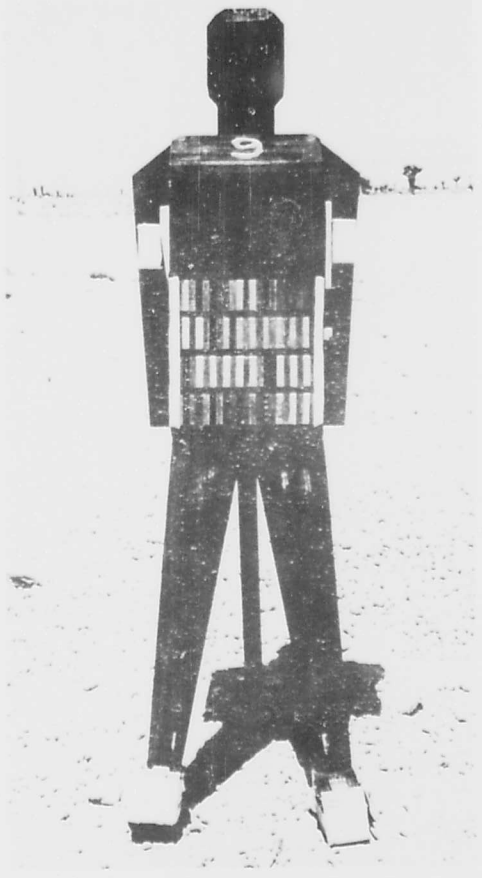

Figure 3.4 Type B simulated human phantom.

Figure 3.5 Set of gold absorber blocks.

Figure 3.6 Kite exposure unit.

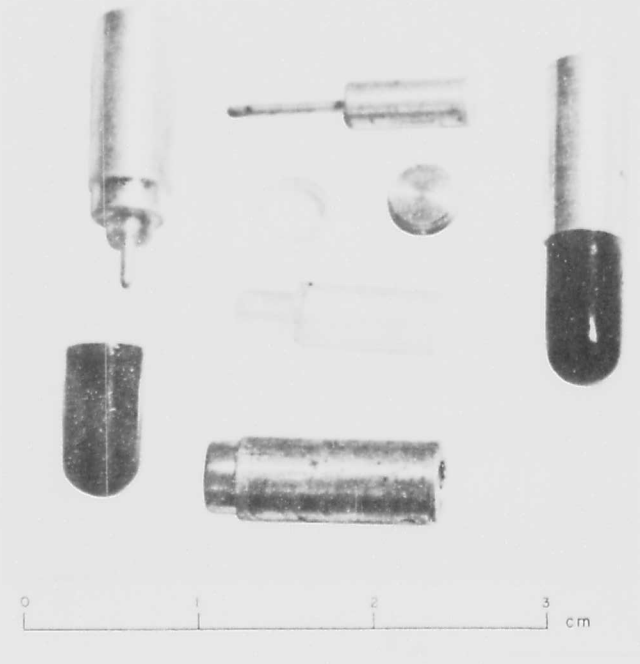

Figure 3.7 Miniature ionization chamber, assembled and disassembled.

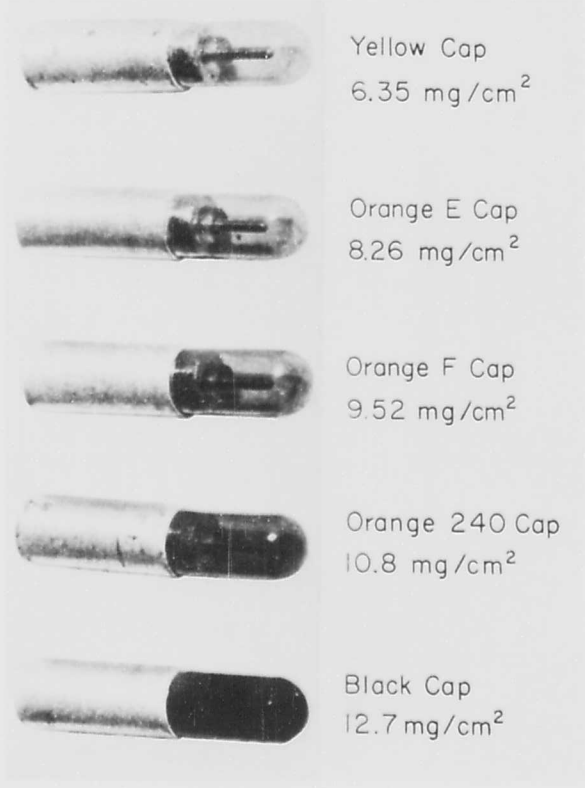

Figure 3.8 Gelatin caps for ionization chamber.

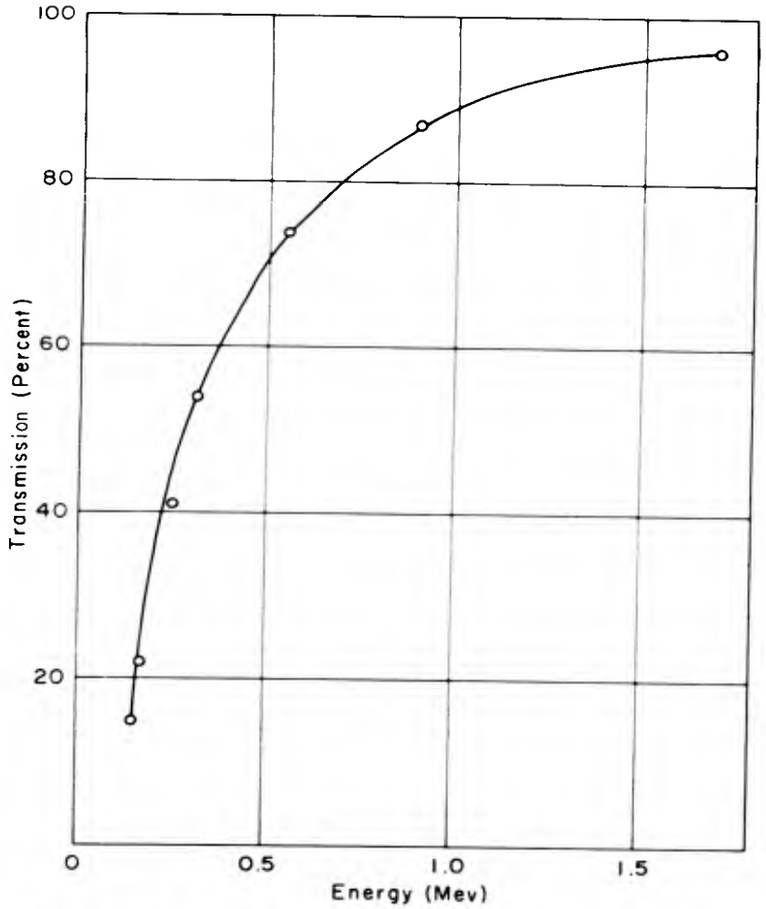

Figure 3.9 Transmitancy of beta radiation through 7 mg/cm^2 of tissue equivalent material with respect to energy.

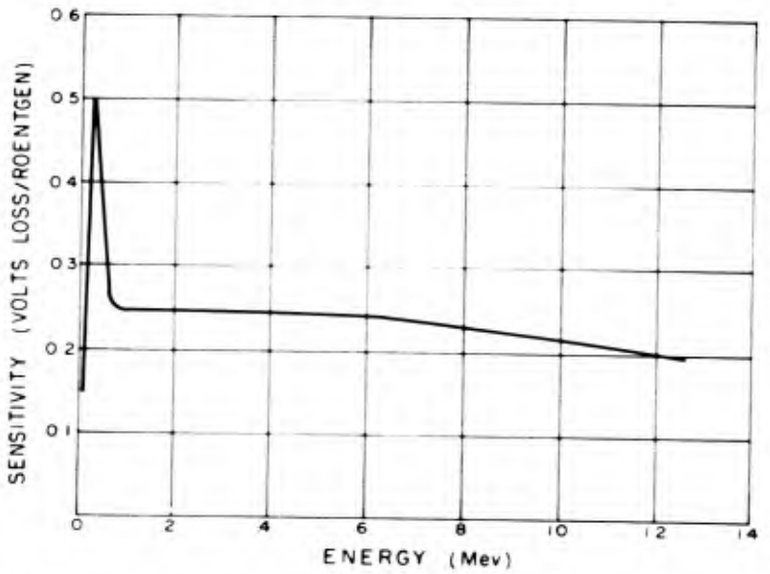

Figure 3.10 Gamma wave length dependence of miniature ionization chamber in free air.

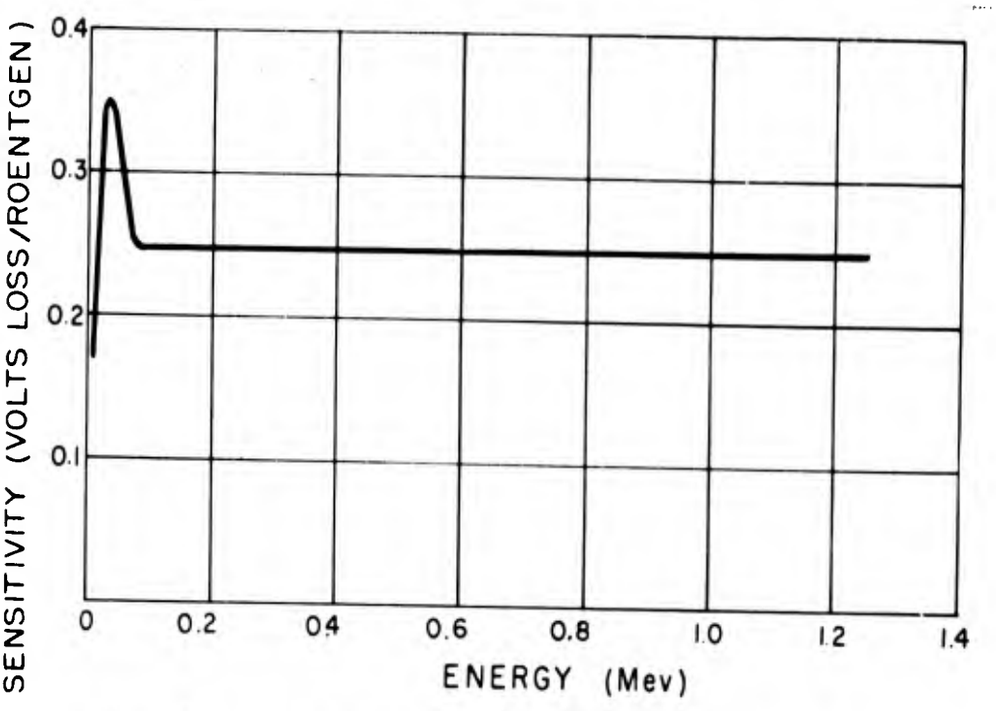

Figure 3.11 Gamma wave length dependence of miniature ionization chamber in masonite block.

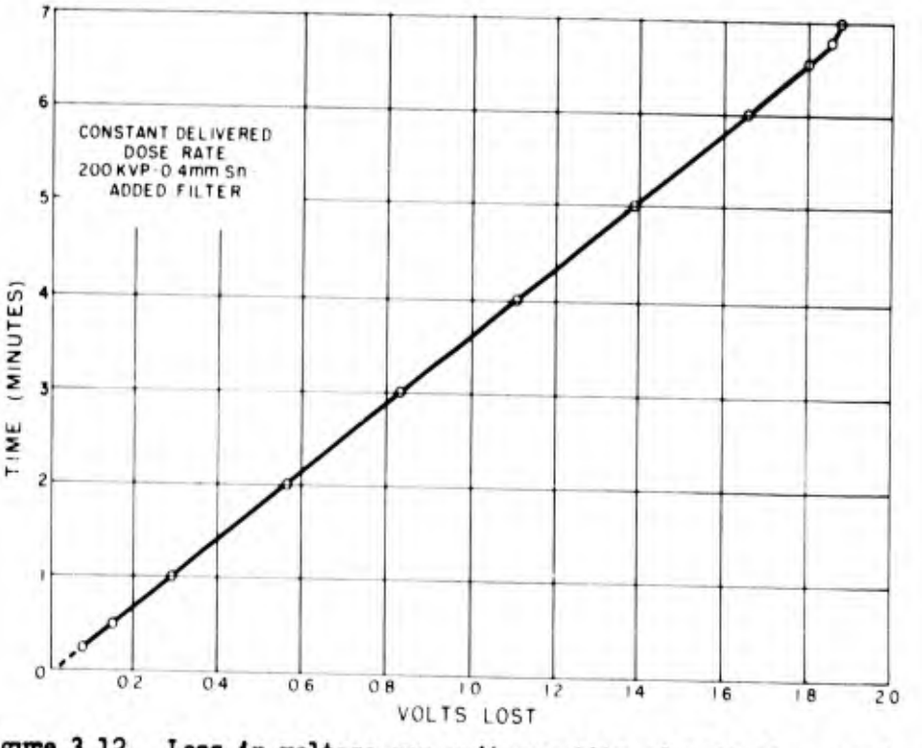

Figure 3.12 Loss in voltage per unit quantity of radiation received.

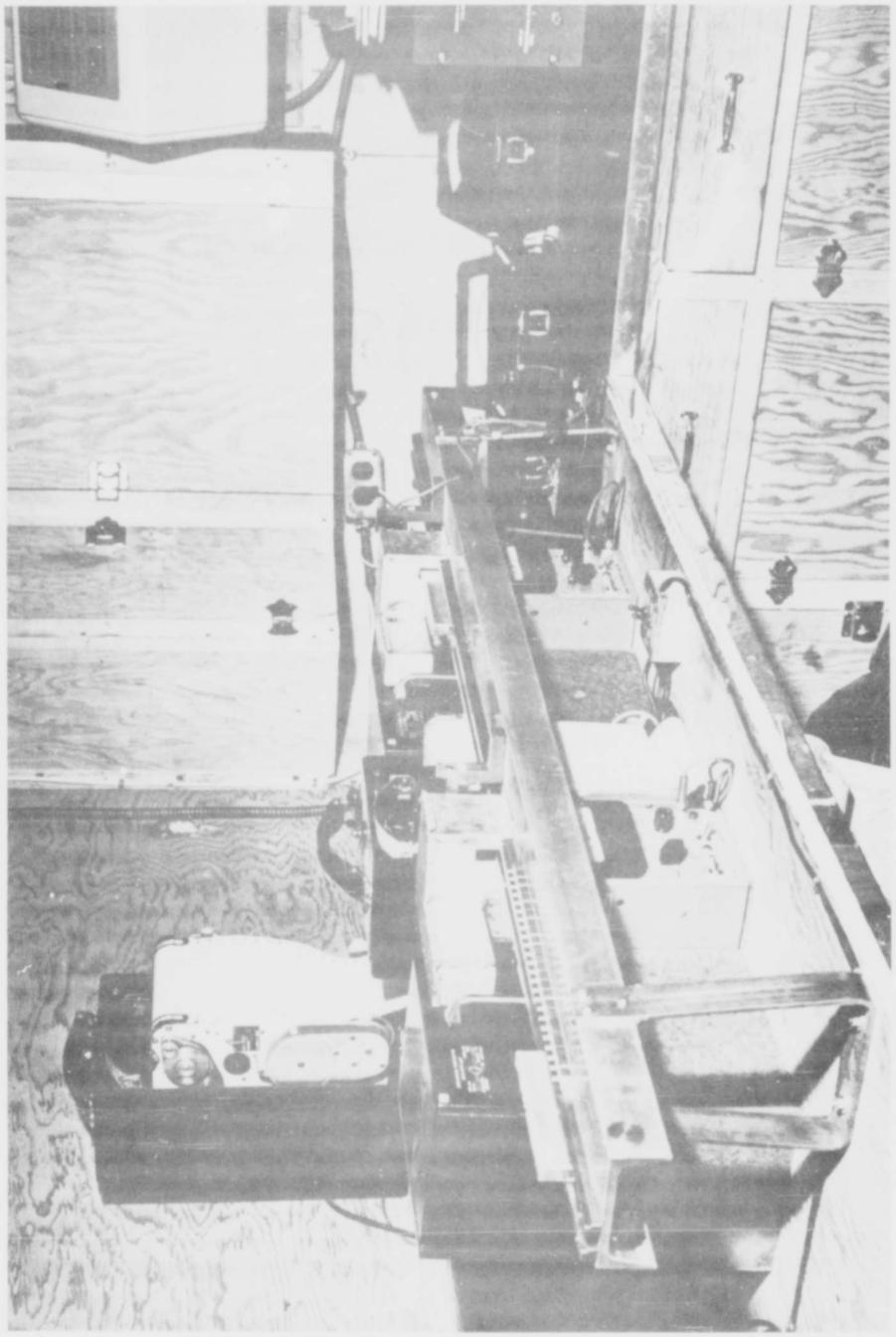

Figure 3.13 Automatic Reader

CHAPTER 4

OPERATING PROCEDURE

4.1 LOADING AND PLACEMENT

Immediately after H-hour all chambers were charged, placed in their designated positions in their phantoms, carried to the field, and placed (Figure 4.1) as soon as the On-Site Rad-Safe Organization would permit entry.

Prior to actual placement of the station, two men preceded the truck carrying the phantoms and located the site of exposure. The fallout area selected was unobstructed by brush, of level terrain, and had a gamma radiation intensity of approximately 2 r/hr at 1 meter from the ground. Radiation intensity measurements were made for both beta and gamma radiation at three different heights from the ground: 38 cm, 67 cm, and 100 cm. The phantoms were then placed in this surveyed area. Table 4.1 lists the actual locations of the various stations for the different shots.

An area of ground approximately 4-by-8 feet was lightly brushed with a board covered by the sleeve of a wool shirt. A Type-A phantom was laid prone over this area (brushed-prone man). The prone man, which was identical in every respect to the brushed-prone man, was placed within a distance of 10 feet. The Type-B phantom (upright phantom) and kite were placed nearby.

4.2 RECOVERY AND READING

After a period of time determined by the 1-meter gamma reading, the station was recovered and returned to the field laboratory for evaluation.

TABLE 4.1 LOCATIONS OF STATIONS FOR EXPOSURE

Shot	Time	Distance from Ground Zero (yards)	Gamma Reading at 1 meter (r/hr)
4	D day	3,000: 0° azimuth	0.6
4	D + 1 day	2,800: 0° azimuth	3.5
4	D + 1 day	2,750: 0° azimuth	3.0
7	D day	3,100: 150° azimuth	1.1
7	D + 1 day	700: 180° azimuth	2.4
7	D + 1 day	630: 180° azimuth	2.3
7	D + 2 days	525: 180° azimuth	2.3
8	D day	2,600: 0° azimuth	1.6

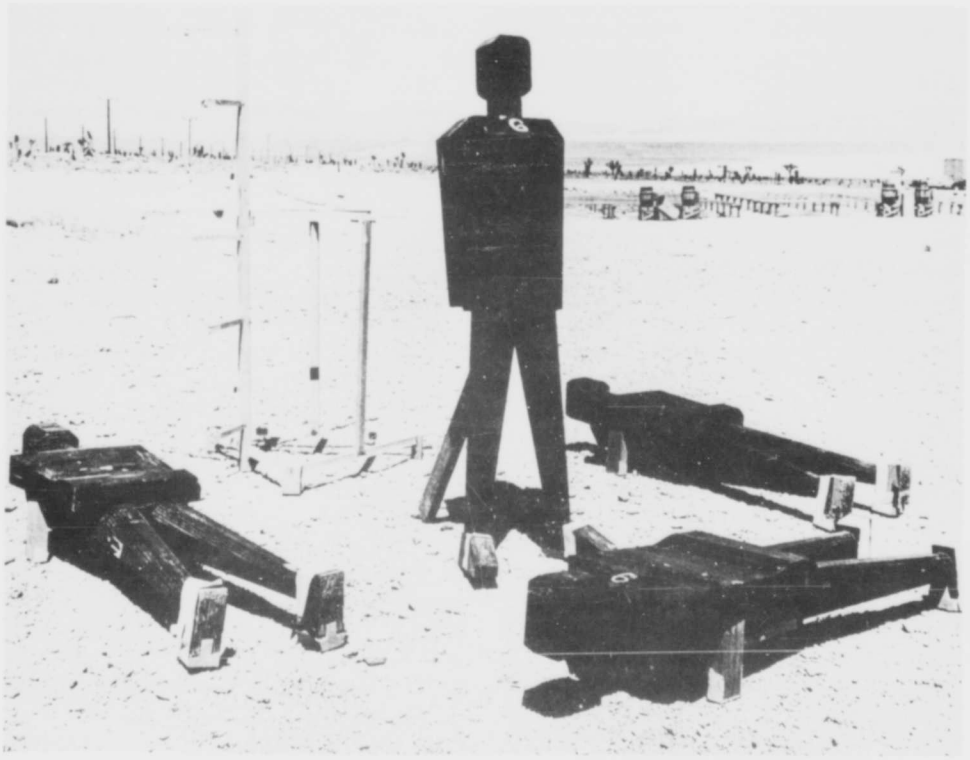

Figure 4.1 Complete station as placed in the field.

CHAPTER 5

RESULTS AND DISCUSSION

5.1 INTRODUCTION

The purpose of this work has been aimed at the determination of energy absorbed, stressing human hazard irrespective of the character, quantity, or quality of the fallout field radiation.

Although much of the data will be given for specific shots, the greatest and most meaningful part of it will be the composite data from several shots.

It would be impractical and cumbersome to report all of the data taken by Project 2.6, since approximately 20,000 ionization chamber measurements were recorded. All of these measurements were used to make the composite data given in this report. However, in the interest of clarity and statistical evaluation, Table 5.1 is a complete copy of one page of the raw, unedited data as it was originally taken.

5.2 UPRIGHT MAN

The human phantom was placed in the fallout field in a standing position, and the dose measurements are illustrated in Table 5.2.

The interior (depth) doses were identical regardless of the site within the upright man. Inasmuch as the thinnest depth dose was completely surrounded by a minimum of 4 cm of tissue equivalent material, no original beta radiation could be present at these locations. Further, since it is known that the multiple scatter processes, created in a low-Z material by almost any energy gamma ray above 0.06 Mev, are such that little attenuation is provided by these low-Z materials, little difference would be expected in dose measurements taken at various depths within the body. However, the importance of the identical readings is the fact that the height above the ground (within the height limits of a man) has no bearing on the dose. Hence, it must be assumed that the bulk of the gamma dose received by an individual from a fallout field originates from the overall active area and not necessarily from where the man is standing and that the radiation from the very immediate vicinity of

TYPE OF RUN Man No. 2: 1st Run

SHOT Ess-D day + 2

TABLE 5.1 TYPICAL ROUGH DATA SHEET

POSITION Prone

DATE March 25, 1955

	Detector and Position	Charging Voltage	Exposure Block Number	Ruler Readings 1	2	3	4	5	Mean	Notes
1	Skin Dose - Nose	355	201	221	244	447	256	-	240	3 readings only
2	" " - Neck, front	355	202	-	148	181	195	192	179	4 " "
3	" " - Chest, sternum	355	203	202	216	207	227	236	218	
4	" " - Navel	355	204	222	202	278	195	-	224	4 " "
5	" " - Upper Femur, front	355	205	273	213	233	239	264	244	
6	" " - Knee	355	206	217	-	236	256	245	238	4 " "
7	" " - Shin	355	207	182	200	168	184	179	183	
8	" " - Abdomen, lower	355	208	213	241	279	349	264	249	4 " "
9	" " - Foot	355	209	123	123	72	136	149	133	4 " "
10	" " - Head, rear	35	210	72	74	69	-	70	71	4 " "
11	" " - Belt, rear		NOT INCLUDED							
12	" " - Upper Femur, rear	35	212	58	64	-	61	66	62	4 " "
13	" " - Back, upper		NOT INCLUDED							
14	" " - Calf, rear	35	214	82	76	71	69	70	74	
15	Depth Dose - Mid Femur, (side)	35	E2	48	60	57	58	60	57	
16	" " - Head, (side)	35	C2	60	65	69	59	67	64	
17	" " - Kidney, (rear)	35	D2	49	48	48	45	52	49	
18	" " - Heart, (rear)	35	B2	61	51	61	57	53	57	
19	" " - Liver, Deep, (rear)	35	A2	62	48	61	36	55	57	4 " "
20	" " - Liver, Shallow, (rear)		NOT INCLUDED							
21	HVL, (mid abdomen) 5 mm. Masonite	355	Front	124	130	-			127	2 " "
22	" " 10 " "	35		73	75	80			76	
23	" " 20 " "	35		66	64	69			66	
24	" " 50 " "	35		54	56	60			57	
25	" " 75 " "	35		51	51	44			49	
26	" " 100 " "	35		48	47	51			49	
27	" " 75 " "	35		49	43	53			48	
28	" " 50 " "	35		55	51	43			50	
29	" " 20 " "	35		48	52	42			47	

the subject may make only a small contribution to the gamma dose received by the individual. This is in contrast to the limited range of beta radiation, which requires that any beta dose received must come from the immediate vicinity of the receiver.

K. Z. Morgan (8) has calculated the dose as a function of height above an infinite plane saturated with gamma emitting contaminates of various energies. The solution of these exponential integrals indicates that the dose 6 feet above the ground should be about 40 percent less than that at 1 foot above the ground. The failure of Project 2.6 to get a difference in the gamma dose, regardless of the point of measurement in the phantom, was probably due to radiation from the ground just below the man passing through a much greater thickness of tissue than radiation which fell normally on the surface. The 500 mg/cm^2 point of Figure 5.6 tends to substantiate this viewpoint, since the data was collected in free air where the only variable was distance from the ground. Regarding this data, it is shown by Figure 5.13 that practically all of the soft component of the total radiation is removed by 500 mg/cm^2 of polyethylene and that radiation still being read must be considered as gamma radiation. Then the dose at 5 cm above the ground is 24 percent higher than that at 100 cm above the ground.

Figure 5.1 is a composite of several shots on different days after the shots showing the percentage of surface dose for each chamber location, taking the average internal dose as 100 percent. It is noteworthy to compare a plot of these values at the respective heights to a normalized curve of vertical air dose readings (Figure 5.2). Figure 5.2 shows that the surface readings of the upright man are in close agreement with the vertical gradation of dose taken on the kite, which indicates that the particular geometry of a man has little effect on the surface dose of radiation received by him from a fallout field.

Since a survey-meter reading is usually taken at waist height, it is interesting to compare the readings for the body extremities with the surface dose reading at waist height. The surface dose of the feet is four times that of the waist, whereas the head surface dose is one-half that of the waist.

In summary, although the internal dose is constant throughout the man and is in fair agreement with that indicated by a normally used survey meter, the surface dose is variable over the body, dependent only upon the distance of the area from the ground; the surface dose can be as much as one order of magnitude higher than the internal dose reading.

5.3 PRONE MAN

The prone man was a Type-A phantom identical with the upright man. As in the case with the upright man, it was found that the interior (depth) doses were the same. Inasmuch as these points are at different depths within the body and are in parts of the body of different shape and exterior size, the gamma depth dose is independent of depth and geometry of the body.

TABLE 5.2 POSITIONS FOR DOSE MEASUREMENTS

Purpose and Position	Height above Ground (cm)
Surface Dose	
Top of Head	180
Nose	167
Rear of Head	167
Neck, front	153
Left & Right Shoulder	133
Chest (sternum)	133
Navel	115
Lower abdomen	97
Upper Femur Front	75
Upper Femur Rear	75
Knee	51
Calf Rear	36
Shin	23
Foot, Outside	6
Interior (Depth) Dose	
Brain	170
Heart	130
Liver	115
Kidney	100
Center of Abdomen	90
Femur (Center of Thigh)	65

The surface dose on the rear side of the prone man is in close agreement with the interior dose, whereas the surface dose readings on the front side were often 20 times higher than the interior doses.

There apparently exists a rapid decay of the soft component of the fallout radiation. This is indicated by the change in the ratio of front surface dose to internal dose in Table 5.3.

TABLE 5.3 TIME VARIATION OF SURFACE DOSE TO INTERNAL DOSE

Time (days)	Ratio (Surface dose to internal dose)
D	20:1
D + 1	10:1
D + 2	5:1

As will be shown later, the penetrating power (energy) of this soft component does not appear to change with time. Therefore, it must be concluded that the mechanism involved is a more rapid decay of the beta emitting isotopes which may be responsible for the high surface dosage than those which are responsible for the gamma component.

5.4 BRUSHED-PRONE MAN

There has been considerable interest in the possible existence of a simple effective means of reducing the radiation hazard incurred when a man is forced to lie in a fallout field of radiation. Such a situation might well develop in the tactical phases of nuclear warfare. Infantry troops might be required to "hit the dirt" for a few minutes at a time; the advisability of this procedure in an area covered with residual fallout radiation is questionable. Project 2.6 has endeavored to evaluate this as a possible hazard.

An area approximately 4-by-8 feet was lightly brushed, as might be done by a soldier with his arms prior to hunching himself forward into that area. The data collected here was compared to the nearby prone man, who was laid over an unbrushed area. The exposure geometries for the brushed-prone and prone men were identical except for the difference created by brushing.

Figure 5.3 shows that approximately 50 percent of the surface dose to the front side of the body can be prevented by this brushing process. In doing this, the internal doses, like the surface doses at the top side of the phantom, are decreased by only about 10 percent, since only a small percentage of the total gamma dose is contributed by areas immediately adjacent to the body in the field. Data taken

from the feet, shoulders, and top of the head were relatively high, since these chambers were essentially directed toward the small pile of contaminated dirt on the periphery of the brushed area as a result of the brushing process.

A reading taken by a normally used radiation survey instrument is much closer to the true surface dose over the brushed area than a reading taken over the non-brushed area.

Although no attempt was made to evaluate the efficiency of brushing an area, certain observations can be made. Brushing can be quite efficient on a sandy, dry area; however, rocky shale or marble-sized gravel presents a difficult condition for brushing efficiency. A smooth surface like concrete or a dry hard lake bed presents a situation in which contamination is not readily removed by brushing.

5.5 KITE

The purpose of the kite was two-fold: (1) to evaluate the change in the penetrating power of the radiation at two distinctly different heights and (2) to determine the air dose variation with height above the ground. These measurements have little or no biological significance, but they do indicate certain physical characteristics of the radiation which will aid in the evaluation of other data of this work.

5.5.1 Absorption Measurements. Absorption studies were made with polyethylene and gold, up to thicknesses of 500 and 3000 mg/cm^2, respectively, at distances of 5 and 100 cm from the ground. Little difference in the slopes of the curves was observed for different shots or different days after the shots. Therefore, for better statistical evaluation, composite curves of the data were made as follows:

1. In a comparison of gold and polyethylene absorption at 5 cm, the slopes of the two curves (Figure 5.4) are substantially identical, indicating that the soft radiation component is probably corpuscular rather than electromagnetic in nature. The difference in attenuation between polyethylene and gold at any particular mass-thickness of absorber is in substantial agreement with the A/Z variation of absorption of beta particles. Concerning a tissue dose, assuming that polyethylene is tissue equivalent, 1 mg/cm^2 is equivalent to a 10-micron thickness of human tissue. An examination of the polyethylene curve shows that the first 1,000 microns of tissue would absorb approximately 40 percent of the total ionization present and the first 2,000 microns of tissue absorbs about 55 percent of the total ionization. Finally, 5,000 microns of tissue is responsible for the absorption of 75 percent of the dose. Since most radiation survey meters in use today have wall thicknesses equivalent to approximately 10,000 microns of tissue, it is apparent that only a small amount of the total absorbed dose is being measured by these instruments.

2. For a comparison of gold and polyethylene absorption at 100 cm, the curve in Figure 5.5 is essentially identical with

Figure 5.4; all statements true of Figure 5.4 apply, with less than 5 percent difference in any of the tissue absorption values.

3. Figure 5.6 presents a comparison of absorption curves in polyethylene at two different heights from the source at 5 and 100 cm.

4. Figure 5.7 compares absorption in gold at two different heights at 5 and 100 cm. These curves, for which enough gold absorbers were utilized to completely absorb the soft component of radiation, show the penetrating power of the radiation in addition to the effect of increased height from the ground. The air dose is approximately six times the hard component dose at 5 cm from the ground. This factor drops to about four at 100 cm. Only the hard component appears to remain after the radiation has penetrated 500 mg/cm^2 of gold.

5. To compare gold and polyethylene absorption at both 5 and 100 cm, Figure 5.8, a composite of Figures 5.4, 5.5, 5.6, and 5.7, is presented.

5.5.2 Vertical Gradation of Dose. Air readings (wall thickness, 8 mg/cm^2) were taken at nine different heights above the ground in order to interpret better the dosage of radiation received at various surface points over the body of an upright man. This data was obtained for two primary reasons: (1) the source was a distributed rather than a point source and (2) the effect upon the dose created by beta radiation as a function of height was not known.

Figure 5.9 is a family of curves from data taken on several shots. The staggering of these lines may be due in part to terrain and other effects encountered in the field.

Figure 5.10 is a composite curve of all the data of Figure 5.9. Also shown is a plot of the inverse square law, in order to point out the radically different type of radiation and source geometry presented by a fallout field. For convenience in expressing the data, both curves in Figure 5.10 were normalized to 100 percent at 100 cm above the ground. From the point of view of human hazard, the variation of dose between the feet and head of an upright man may be about a factor of five.

5.6 ABSORBER MAN

Absorption studies were made, not in a particular effort to determine energy, but rather to evaluate better the characteristics of the radiation in terms of tissue penetration. However, in so doing this study has provided much information regarding the physical character of the radiation.

5.6.1 Radiation Absorption in Tissue Equivalent Material for Several Shots. An examination of Figure 5.11 shows that the character of the radiation of several shots on several different days follows essentially the same attenuation through 500 mg/cm^2 of tissue equivalent material. To suffer this degree of attenuation through the equivalent of 5,000 microns of tissue, the radiation must be soft, but nevertheless damaging. The shape of the curves does not answer the question as to whether or not this radiation is beta or gamma radiation.

If gamma, it must be quite soft (~ 10 kev), in order to be attenuated by so little mass. On the other hand, one would surmise a 1-to-2 Mev beta, if it can be shown that this radiation is corpuscular in nature.

5.6.2 Copper Absorption of Radiation for Different Shots on Different Days. This data (Figure 5.12) is presented to show the thickness of material required to absorb completely the soft component of radiation that is not usually measured with a field survey instrument. This curve shows complete absorption of the soft component by about 700 mg/cm^2 of copper. If this soft component is assumed to be beta radiation, rather than soft gamma rays, then 700 mg/cm^2 of copper is in fair agreement with the stopping power of 700 mg/cm^2 (7,000 microns) of tissue. At any given thickness, the extremes of variability in dose readings do not exceed ± 30 percent of the mean.

5.6.3 Composite Absorption Curves. Composite curves (Figure 5.13) were made for the attenuation of radiation by each metal from a group of curves of individual shots, such as Figures 5.11 and 5.12. These composites were then plotted on one graph in order to compare the attenuation of the radiation by different metals. The curves show close similarity of the absorption processes regardless of the Z-number of the absorber. Only gold and copper absorbers were used in thicknesses sufficient to absorb all the remaining soft component.

The gamma component of the curves, 800 mg/cm^2 to 3,000 mg/cm^2, show that the energy of this radiation is sufficiently hard so that tissue in any normally found body thickness will cause negligible variation in dose within the body. The ratio of surface to depth dose is about six to one.

Figure 5.14 is a plot of the data of Figure 5.13, with the gamma component subtracted in order to consider the soft component separately. These curves are quite characteristic of beta-particle absorption. Beta-radiation attenuation is relatively independent of the atomic number of the absorber, being primarily a function of mass per unit area. The dependence of beta-particle absorption on atomic number varies roughly as the ratio of atomic weight to atomic number (A/Z). Hence, beta absorption by heavy elements is expected to be slightly greater per unit mass than by light elements. Figure 5.14, within the accuracy of this experiment, shows that such a rule is followed.

5.7 LOW-ENERGY COMPONENT OF RADIATION

The discussion in Chapter 2 pointed out that from a biological standpoint it makes relatively little difference to dosage measurements and human hazard whether the soft component of fallout radiation is beta particles or soft gamma radiation. This is not true in the case of instrumentation. Though gamma radiation is recorded as a result of the secondary electrons produced by gamma interaction with matter, the quality and quantity of those secondaries produced is dependent on the construction and composition of the detector walls. This is not true

in the case of beta radiation. Hence, a knowledge of whether one must measure beta or soft gamma radiation has a definite bearing on the design of instruments to evaluate properly the activity of this radiation.

Further, while not of specific interest in evaluating human dosage, a knowledge of the energy of this soft component is helpful in the design of instruments and particularly useful to the biologist to provide a simulated source of this radiation for laboratory measurements. Therefore, Project 2.6, with the cooperation of the Oak Ridge National Laboratory, set up an energy-calibration system for beta-radiation exposure. As far as practicable, every effort was made to duplicate exactly the geometry of exposure, using a distributed source of radiation such as that found in a fallout field. Large sheets of filter paper were saturated uniformly with a solution of pure beta-emitting radioactive material. After drying and making an assay of the quantity of isotope on each sheet (usually about 100 $\mu c/cm^2$), these sheets were spread over the ground, covering an area of approximately 4 by 8 feet. For beta radiation the center of the area was essentially equivalent to an infinite plane source of beta radiation.

The human phantoms and the kite were exposed at the center of this area exactly as they were exposed in a fallout field. It was intended that data derived by this calibration system could duplicate, in so far as possible, the beta radiation within a fallout field.

The isotopes used and their energies are shown in Table 5.4.

TABLE 5.4 ISOTOPE ENERGIES FOR CALIBRATION

Isotope	Energy (Mev)
Pd^{109}	0.95
P^{32}	1.70
Y^{90}	2.20

Figures 5.15 through 5.19 present a comparison of P^{32} data for various metal absorption systems in the absorber man. The similarity between the apparent energy of the soft component of fission fallout radiation and the beta radiation of P^{32} is evident. The field data in each case is a composite of all shots for that particular metal. The gamma component is subtracted as in Figure 5.14. In each case, the field data indicates a slightly softer radiation than P^{32} up to approximately 100 mg/cm^2, at which point it tends to become slightly harder than the 1.7 Mev beta radiation of P^{32}. Effectively, however, the curves indicate a beta-radiation energy quite close to that of P^{32}. Figure 5.20, which is a composite of all the absorption curves of each metal combined into one curve, is presented to show how closely similar the field radiation energy is to that of P^{32}, 1.7 Mev.

The determined half-value thickness of the radiation in each metal absorbing system is further support of the opinion that the bulk of the soft component of fallout radiation is corpuscular rather than electromagnetic in nature.

in the case of beta radiation. Hence, a knowledge of whether one must measure beta or soft gamma radiation has a definite bearing on the design of instruments to evaluate properly the activity of this radiation.

Further, while not of specific interest in evaluating human dosage, a knowledge of the energy of this soft component is helpful in the design of instruments and particularly useful to the biologist to provide a simulated source of this radiation for laboratory measurements. Therefore, Project 2.6, with the cooperation of the Oak Ridge National Laboratory, set up an energy-calibration system for beta-radiation exposure. As far as practicable, every effort was made to duplicate exactly the geometry of exposure, using a distributed source of radiation such as that found in a fallout field. Large sheets of filter paper were saturated uniformly with a solution of pure beta-emitting radioactive material. After drying and making an assay of the quantity of isotope on each sheet (usually about 100 $\mu c/cm^2$), these sheets were spread over the ground, covering an area of approximately 4 by 8 feet. For beta radiation the center of the area was essentially equivalent to an infinite plane source of beta radiation.

The human phantoms and the kite were exposed at the center of this area exactly as they were exposed in a fallout field. It was intended that data derived by this calibration system could duplicate, in so far as possible, the beta radiation within a fallout field.

The isotopes used and their energies are shown in Table 5.4.

TABLE 5.4 ISOTOPE ENERGIES FOR CALIBRATION

Isotope	Energy (Mev)
Pd^{109}	0.95
P^{32}	1.70
Y^{90}	2.20

Figures 5.15 through 5.19 present a comparison of P^{32} data for various metal absorption systems in the absorber man. The similarity between the apparent energy of the soft component of fission fallout radiation and the beta radiation of P^{32} is evident. The field data in each case is a composite of all shots for that particular metal. The gamma component is subtracted as in Figure 5.14. In each case, the field data indicates a slightly softer radiation than P^{32} up to approximately 100 mg/cm^2, at which point it tends to become slightly harder than the 1.7 Mev beta radiation of P^{32}. Effectively, however, the curves indicate a beta-radiation energy quite close to that of P^{32}. Figure 5.20, which is a composite of all the absorption curves of each metal combined into one curve, is presented to show how closely similar the field radiation energy is to that of P^{32}, 1.7 Mev.

The determined half-value thickness of the radiation in each metal absorbing system is further support of the opinion that the bulk of the soft component of fallout radiation is corpuscular rather than electromagnetic in nature.

As mentioned in Section 5.6.3, the first half-value layer of the radiation in each metal was determined and normalized to a calculated half-value layer on the copper figure, resulting in the data given in Table 5.5.

TABLE 5.5 CALCULATED VERSUS MEASURED HALF-VALUE LAYER

Material	Calculated HVL (mg/cm^2)	Measured HVL (mg/cm^2)
Polyethylene	67	76
Aluminum	64	68
Copper	60	60
Tin	56	40
Gold	53	50

Considering that the A/Z rule is little more than an approximation, the agreement of the field half-value layers with the calculated half-value layers is striking. To further justify these statements, calculated half-value layers for gamma radiation are cited from White (9) in Table 5.6.

TABLE 5.6 HALF-VALUE LAYERS

Energy (kev)	Polyethylene mg/cm^2	Aluminum mg/cm^2	Copper mg/cm^2	Tin mg/cm^2	Gold mg/cm^2
10	146	[illegible]	[illegible]	6	10
15	462	[illegible]	[illegible]	13	5
20	[illegible]	[illegible]	21	39	11
25	[illegible],955	342	64	17	34

The half-value layers in each metal as shown in Table 5.6 would indicate the following gamma ray energies:

TABLE 5.7 INDICATED GAMMA RAY ENERGIES BASED ON TABLE 5.6 DATA

Material	Energy (kev)
Polyethylene	8
Aluminum	13
Copper	29
Tin	21
Gold	35

It is highly doubtful that the accuracy of the absorption data taken by this project could be so greatly in error as to not be able to differentiate an 8-kev gamma ray from a 35-kev gamma ray.

5.8 SURFACE VERSUS INTERNAL DOSE

As discussed in Section 5.3, the internal doses of the prone man were essentially the same regardless of the internal site of the measurements. The surface doses on the under side of the prone man from chest to shin were equidistant from the ground and hence were identical. Therefore, ratios of the average of these particular surface doses to the average of the internal doses, should be reliable surface to internal dose ratios. Table 5.8 lists the calculated surface to internal dose ratios for several situations.

TABLE 5.8 SURFACE TO INTERNAL DOSE RATIOS

Shot and Time	Ratio
Shot 4, D day	9:1
Shot 4, D + 1 day, 1st Run	7:1
Shot 4, D + 1 day, 2nd Run	2:1
Shot 7, D day	2:1
Shot 7, D + 1 day, 1st Run	2:1
Shot 7, D + 1 day, 2nd Run	1:1
Shot 7, D + 2 days	2:1
Shot 8, D day	4:1

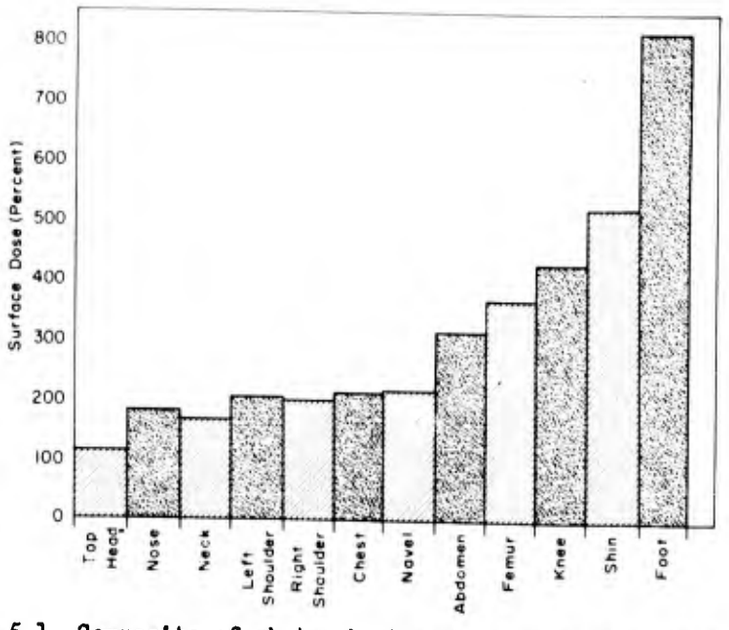

Figure 5.1 Composite of shots showing percentage of surface dose using average internal dose as 100 percent for an upright man.

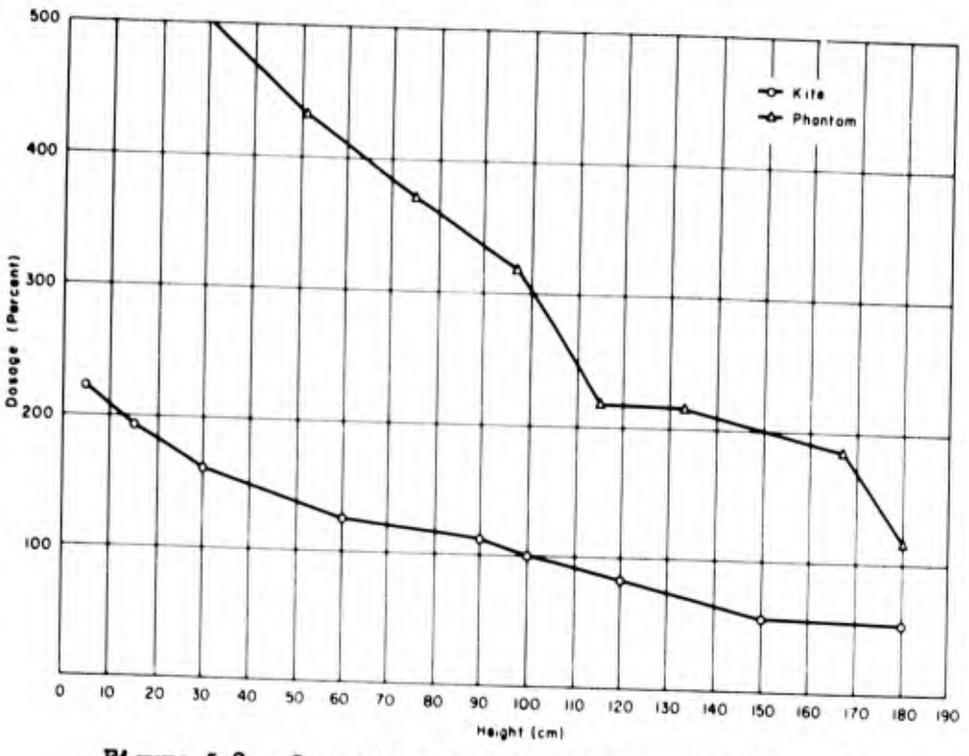

Figure 5.2 Composite of shots showing percentage of surface dose using average internal dose as 100 percent and normalized vertical air dose readings.

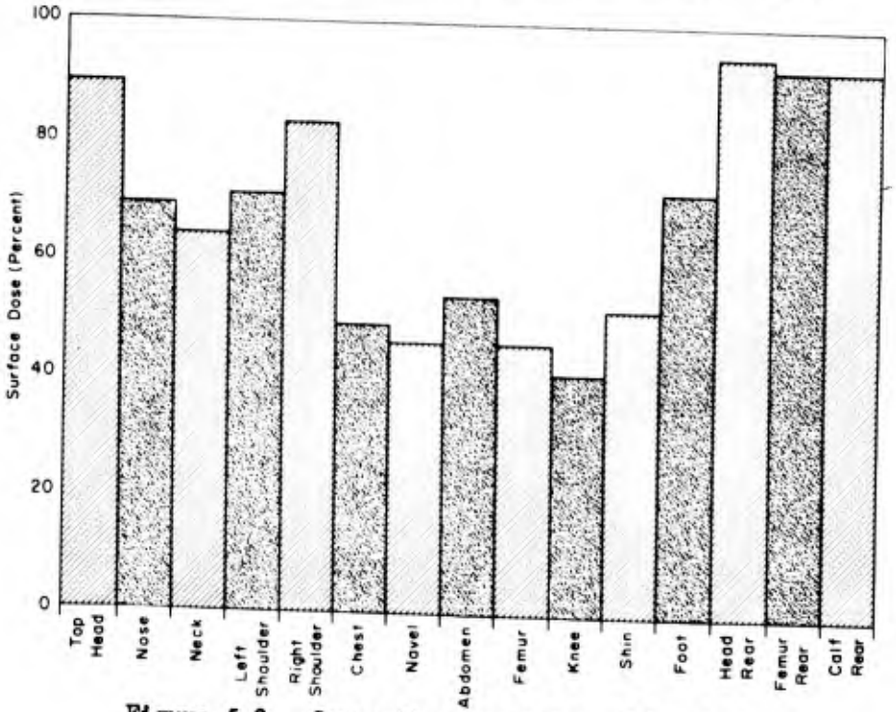

Figure 5.3 Composite percentage of brushed surface dose to non-brushed surface dose.

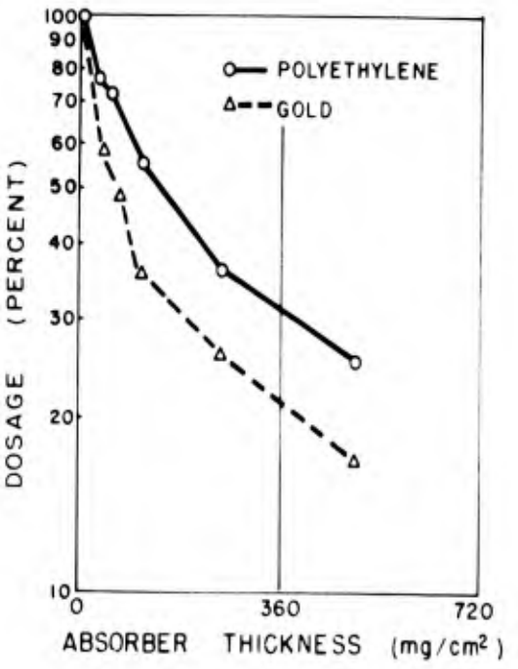

Figure 5.4 Gold and polyethylene absorption in air at 5 cm.

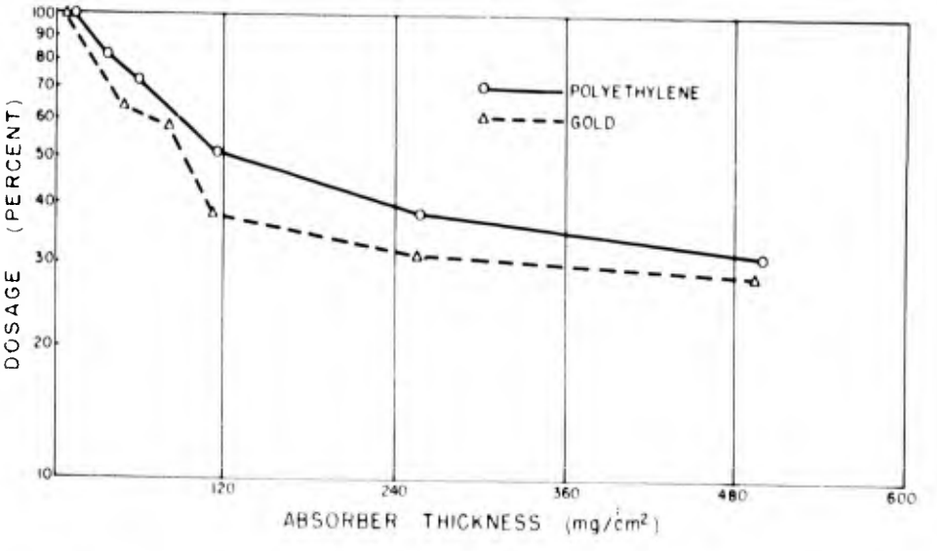

Figure 5.5 Gold and polyethylene absorption in air at 100 cm.

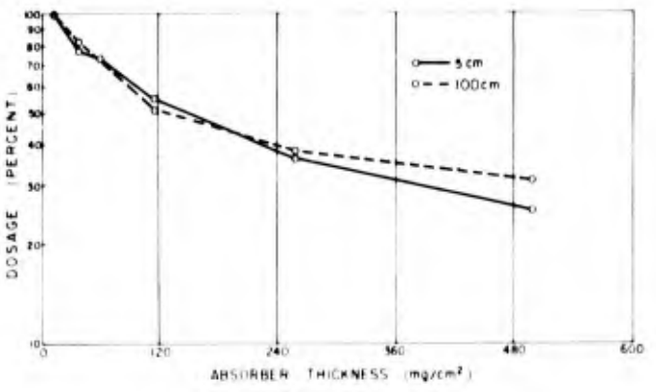

Figure 5.6 Polyethylene absorption in air at 5 cm and 100 cm.

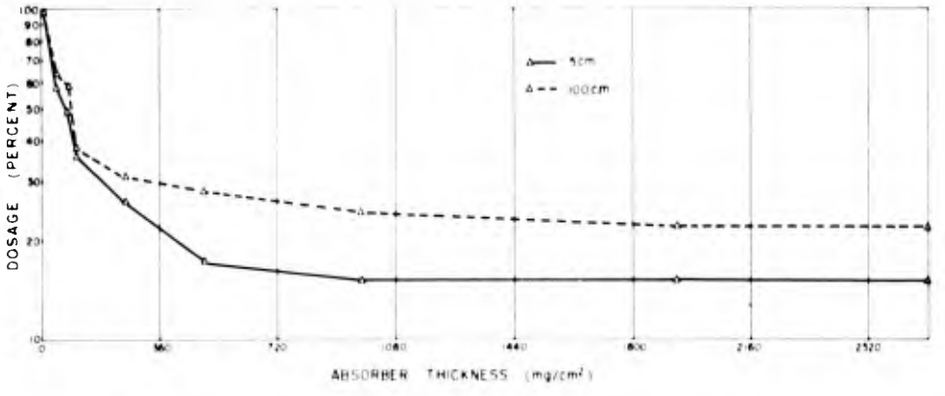

Figure 5.7 Gold absorption in air at 5 cm and 100 cm.

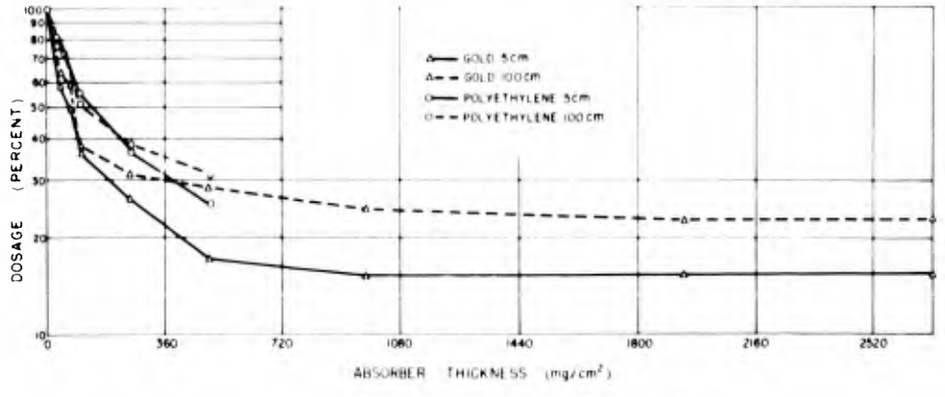

Figure 5.8 Composite absorption of gold and polyethylene at 5 and 100 cm.

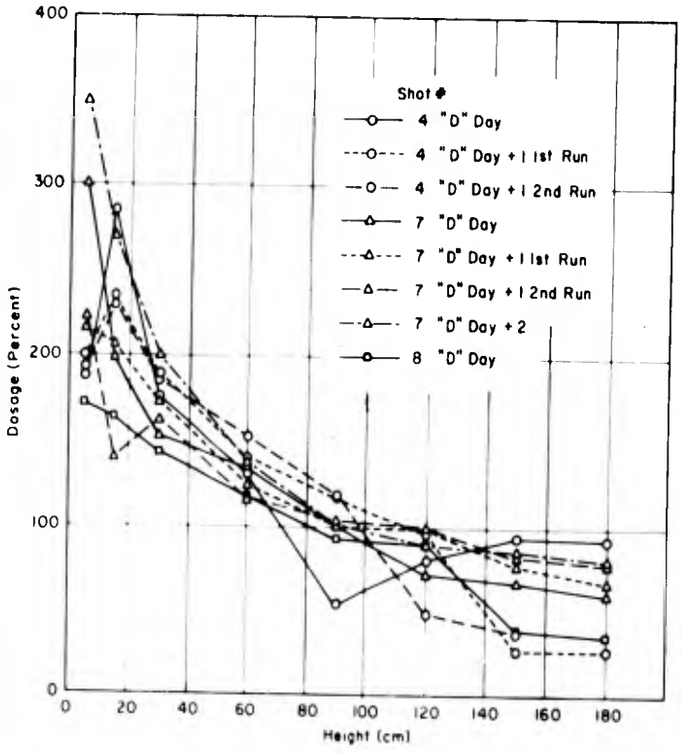

Figure 5.9 Vertical gradation of air dose.

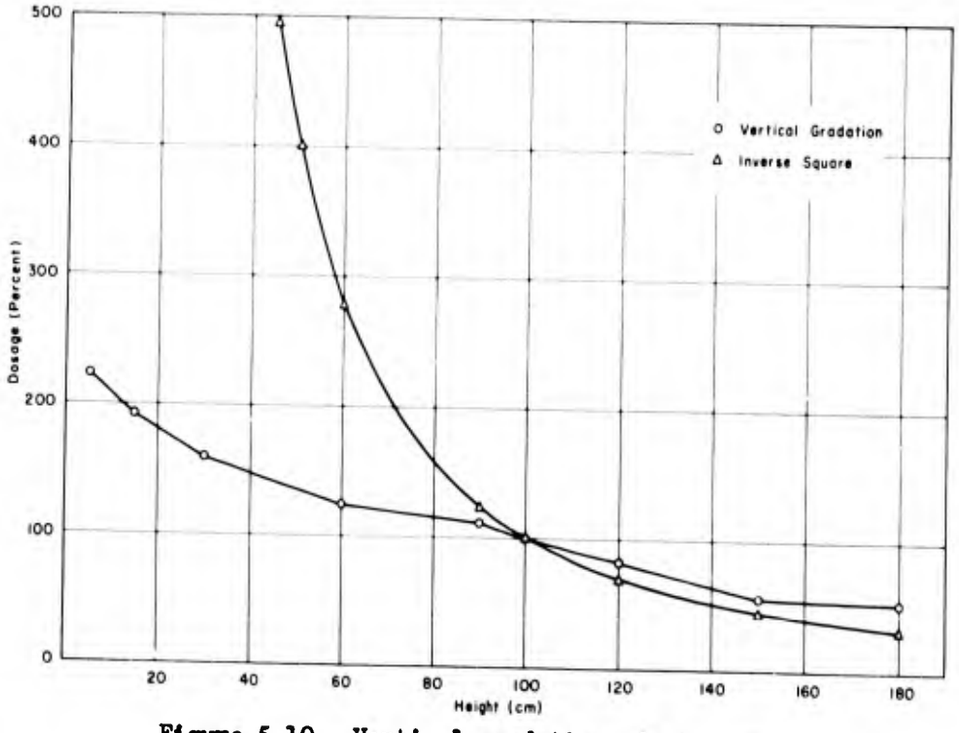

Figure 5.10 Vertical gradation of air dose compared with inverse square law curve.

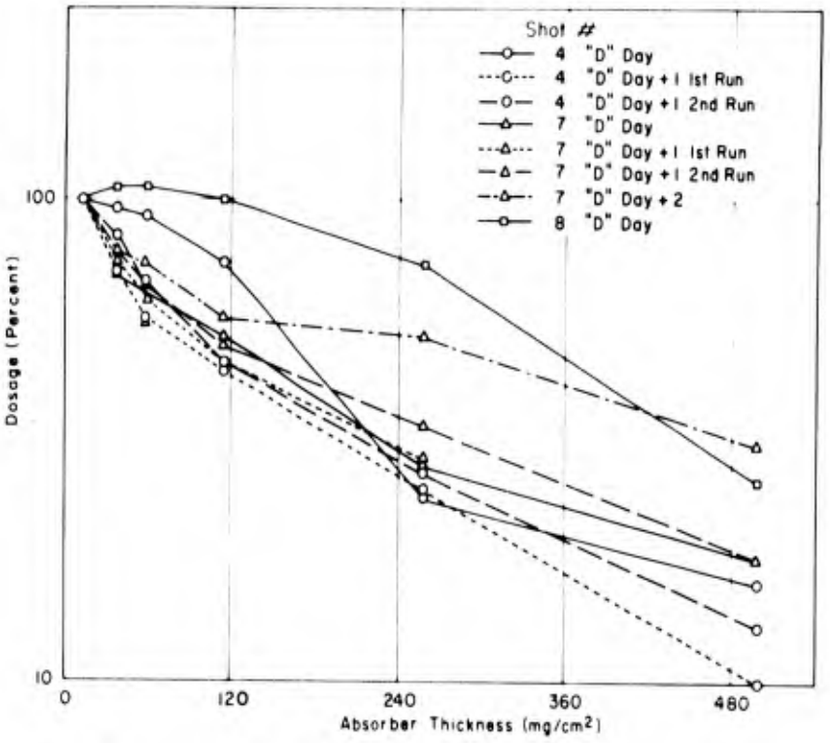

Figure 5.11 Composite polyethylene absorption curves.

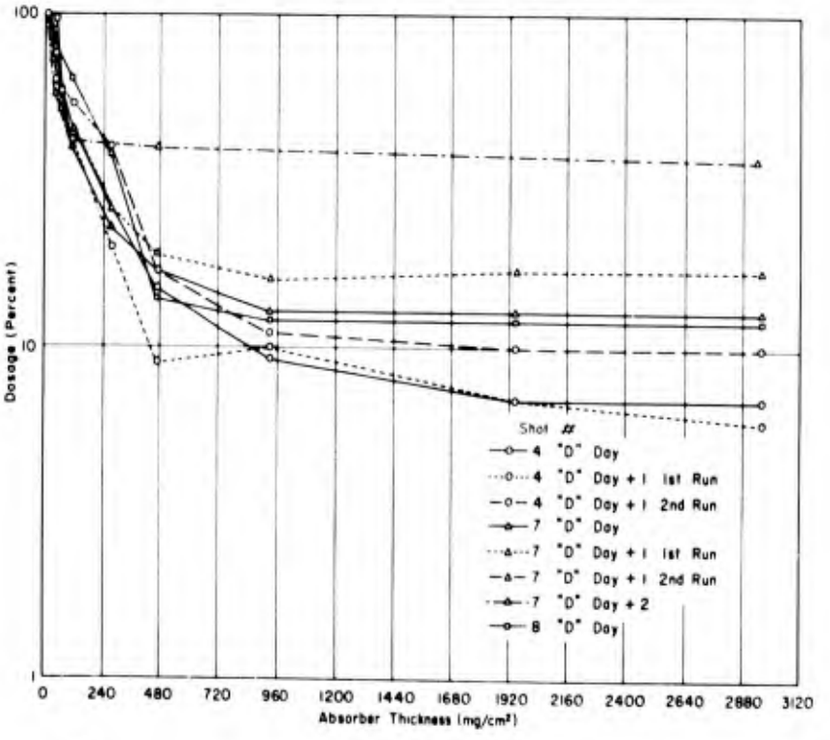

Figure 5.12 Composite copper absorption curves.

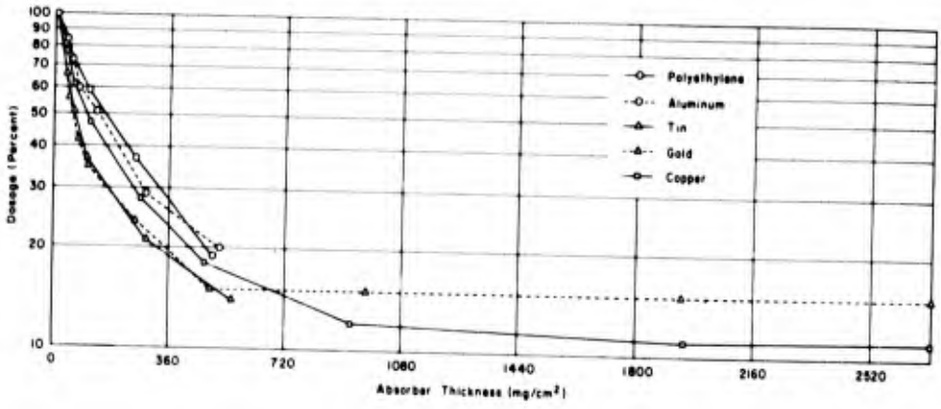

Figure 5.13 Composite absorption curves.

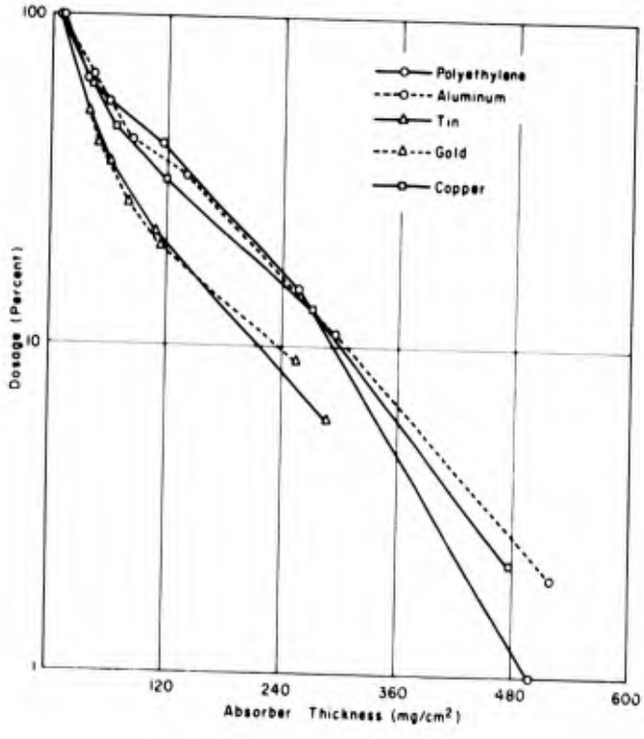

Figure 5.14 Composite absorption curves minus gamma component.

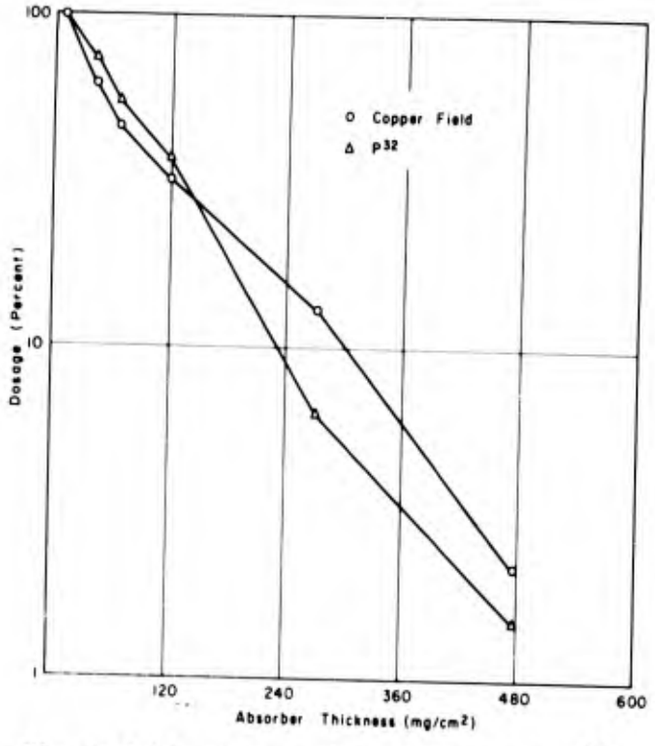

Figure 5.15 Copper absorption versus P^{32}.

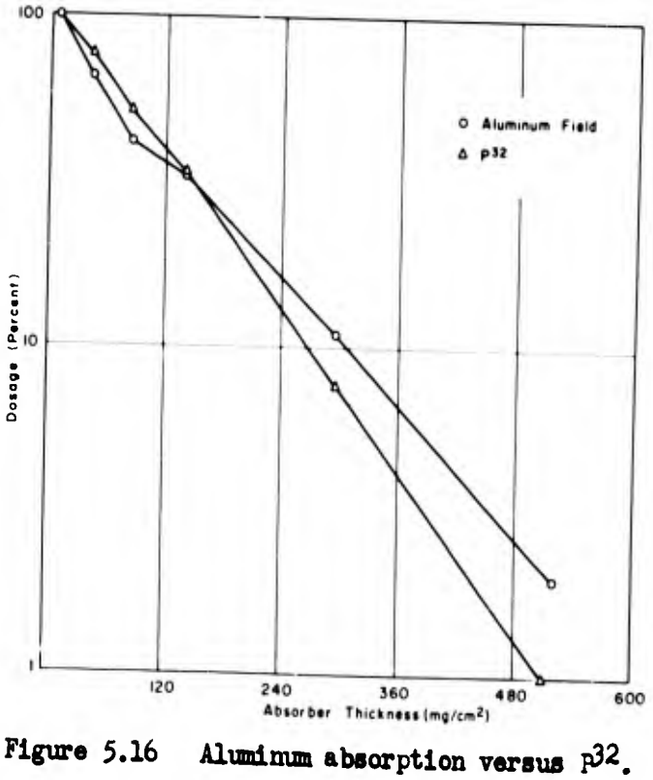

Figure 5.16 Aluminum absorption versus P^{32}.

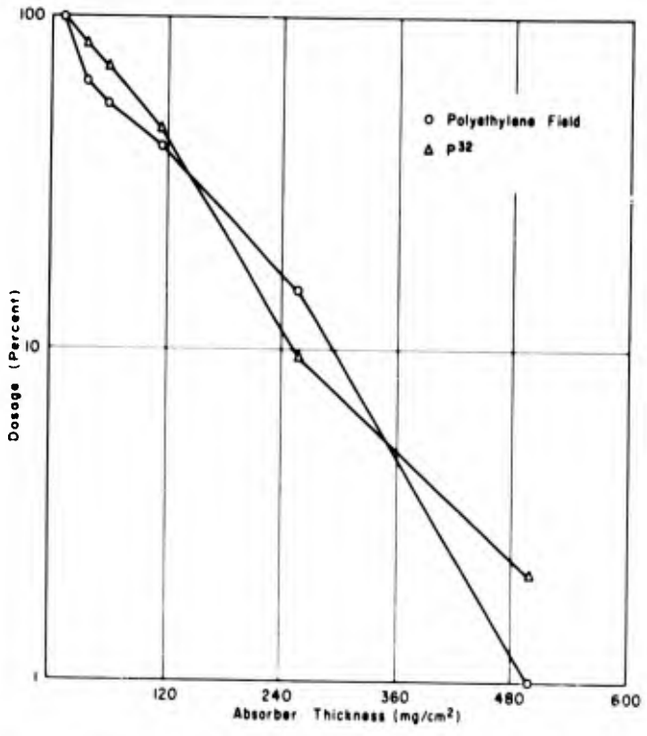

Figure 5.17 Polyethylene absorption versus P^{32}.

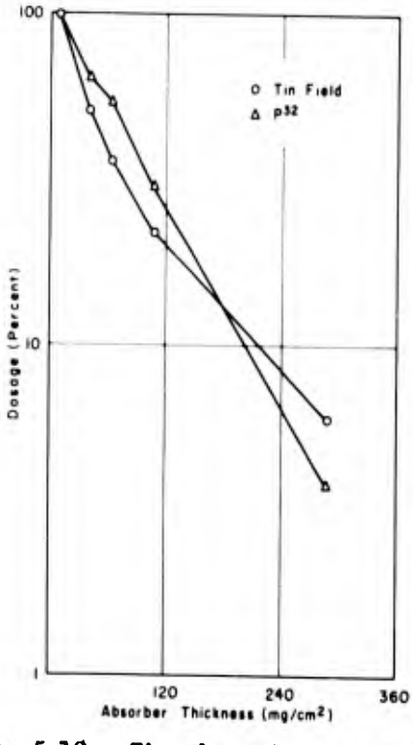

Figure 5.18 Tin absorption versus P^{32}.

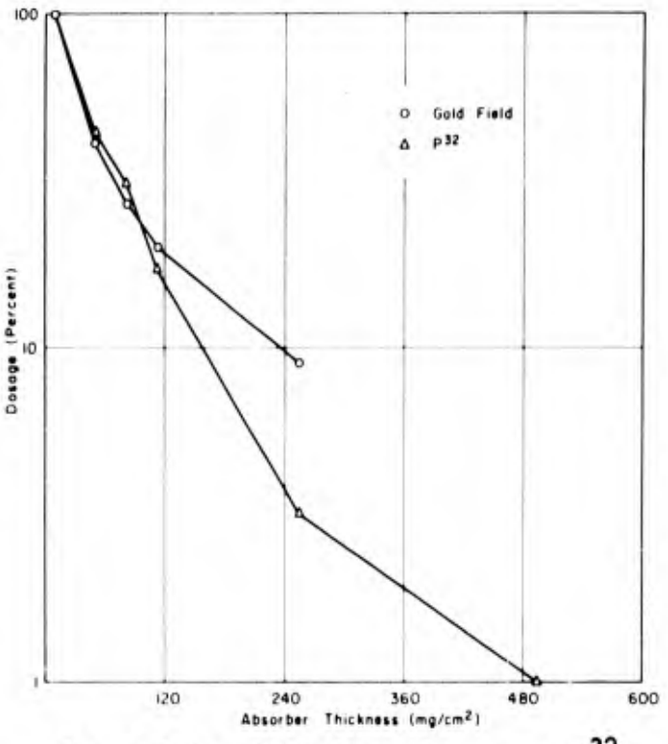

Figure 5.19 Gold absorption versus P^{32}.

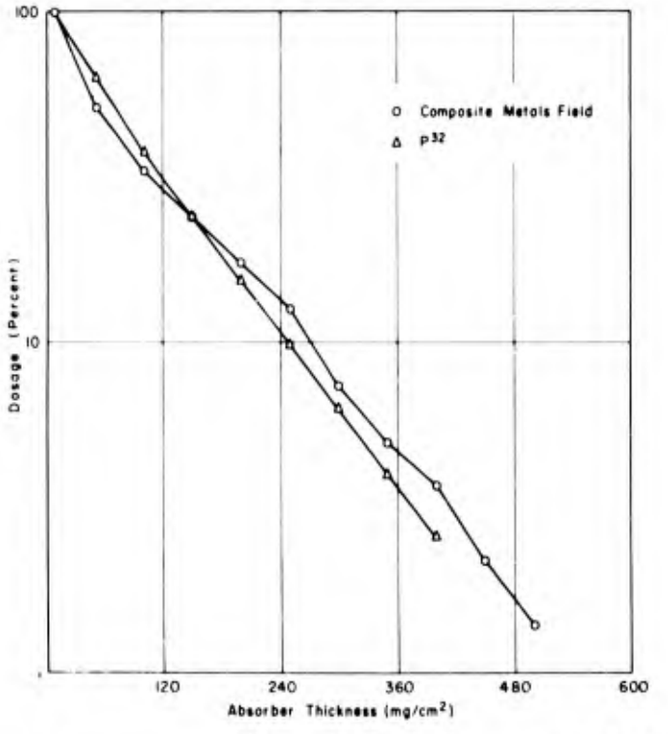

Figure 5.20 Composite metal absorption versus P^{32}.

CHAPTER 6

INFLUENCE OF GEOMETRY ON OBSERVED DOSAGE

After participation in Shots 4, 7 and 8, from which the data of this report is taken, it became apparent that the geometry of the chambers might not be representative of an actual point on the surface of a human body. Therefore this was checked on Shot 13. The results are given in this chapter.

6.1 THEORETICAL GEOMETRY

The masonite block, (Figure 3.2) described in Section 3.2 was used as the ionization chamber holder for all data taken for this report. An inspection of a cross sectional scale drawing, (Figure 6.1), of this confined chamber illustrates the limited solid angle of geometry presented to soft radiation.

Considering the tip of the antenna (A) is the effective electrical center of ionization within the chamber, then the solid angle (XAY) defines the geometry of this arrangement to non-penetrating radiations. If the total solid angle about a point is defined as 4π steradians, then the geometry of this chamber in its holder subtends a solid angle of 31 percent of 2π steradians. This figure is calculated on the basis that the distance of the tip of the antenna under the surface of the block is 2.5 mm and the radius of the hole in the masonite block is 2.6 mm.

Figure 6.2 illustrates the effect of this geometry factor on the measurements of surface dosage as reported in the preliminary report of this project.

A distance of 5 cm between the ground and phantom surface was the closest distance used in any measurement. Angle XAY defines an area (MN) on the ground of 94 cm^2. A soft radiation originating at point Z and traveling directly towards point A will be effectively blocked from entering the chamber due to the masonite walls of the exposure block. Obviously the parameters of material thickness in this entire consideration are such that this discussion is true only for beta radiation. Gamma radiation of almost any energy would not be shielded from entering the chamber by the few millimeters of masonite which comprise the edge of the exposure block.

6.2 EXPERIMENTAL GEOMETRY

A masonite block loaded with one ionization chamber was placed 5 cm above a point source of P^{32}. Measurements were made with this chamber when the source was moved various horizontal distances from the perpendicular projection of the center of the chamber. This arrangement is shown in Figure 6.3.

The experiment was repeated in all details except that the masonite block was removed, leaving the chamber open from all directions. Figure 6.4 contrasts the results and clearly points out the "limiting" effect of the masonite block to beta radiation as this geometry was used in the field.

6.3 FIELD STUDY

Groups of five chambers were placed at each point of data collection over the human phantom. These chambers were placed longitudinally in contact with the body surface and as close as practical to the normally used masonite block chambers. Only two phantoms were used in this experiment, one upright and the other in a prone position.

Since the absolute readings are unimportant the data is given in Table 6.1 in terms of the ratio of the open chambers to the reading of normally used masonite block chambers.

Since this new interpretation of surface dose substantially changes all of the data presented in this report it was deemed advisable to make an absorption study with these "open chambers." Sheets of polyethylene film were laid over the group of five detectors and the unit taped to the front surface of a prone man (Figure 6.5).

The results of this absorption study are graphically given in Figure 6.6. The slopes of these curves are in excellent agreement with those of Figure 5.11, and hence it is felt that the "restricted geometry" in no way effected the estimation of the penetrating power of this soft component.

A further effort was made to clarify the data by the use of lucite caps (Figure 6.7) to determine the absorption of radiation from a fission fallout field. These caps varied in wall thickness from 0.5 mm to 16 mm, or a range of 59 to 1,888 mg/cm^2. In order to eliminate any geometry effect produced by the varying physical size of the lucite caps themselves, these measurements were made 100 cm above the ground. The results are graphically shown in Figure 6.8.

6.4 SIGNIFICANCE

It must be realized that the work described in this chapter was performed only on Shot 13, since the role played by chamber geometry was not fully appreciated until after data was taken on Shots 4, 7 and 8. As stated in Chapter 5, there appeared to be little change in radiation quantum energy between D day and D + 2 days, and the shift in beta to gamma ratio was not drastic during this time. Further, it appeared that the differences in field quantum energy and beta to gamma ratio with respect to the shots participated in were small.

TABLE 6.1 RATIO OF UNRESTRICTED TO RESTRICTED GEOMETRY

Phantom	Ratio, Open Chamber to Restricted Chamber			
	D day	D + 1 days	D + 2 days	Average
Prone man				
Nose	2.38			
Neck	2.12			
Chest	2.22			
Navel	2.21			
Abdomen	1.91			
Femur	2.59			
Knee	1.84			
Shin	1.49			
Foot	3.06			
Average	2.31			
Prone man, rear				
Head	1.10			
Femur	1.03			
Calf	1.16			
Average	1.10			
Upright man				
Nose	3.23		3.11	3.17
Head, rear	3.25	3.52	2.80	3.19
Neck	3.14		2.72	2.93
Chest	3.21		2.84	3.03
Navel	3.25		3.00	3.13
Lower Abdomen	2.23		2.26	2.25
Femur	2.34	2.57		2.45
Femur, rear	2.44	2.29		2.37
Knee	2.93	2.90		2.92
Shin	2.48	2.71	3.51	2.90
Calf	2.02	2.20	2.72	2.31
Foot	2.18	2.45	3.24	2.62
Average	2.73	2.66	2.91	2.77

Thus, it would seem plausible that certain data presented in this report should be corrected or modified by the results of the work described in this chapter.

The calculated figure of 31 percent of 2 π steradians given in Section 6.1 can be converted into a factor of 3.22 for comparison with the experimental determined factors. This calculated value of 3.22 is higher than those found experimentally because the calculated factor is based on a pure beta-radiation source, whereas the experimental factors have a constant gamma radiation component.

An analysis of the three different beta-radiation geometries presented in this discussion indicates a difference in beta-gamma ratio in the order anticipated, (Figure 6.9). All three conditions are subject to recording the same gamma radiation dose, because of the high penetrating power of this radiation present. However, the normally used chambers "see" a restricted beta radiation field, the polyethylene-covered chambers in contact with the down side of a prone phantom "see" a 2 π beta field, while the lucite-capped chambers "see" nearly a 4 π beta field. Little difference would be expected between the polyethylene-covered chambers and the lucite-capped chambers, since little beta radiation will approach a detector from the top hemisphere of a 4 π condition when the activity is confined to the ground itself.

The authors feel that it would not be justifiable to modify all the data of this report by the information reported in this chapter, inasmuch as this would introduce a controversy regarding the degree of validity one might attach to the work of this project. However, the authors are of firm opinion that all the surface doses reported should be elevated by a factor of approximately 2.5 in order to provide a more realistic estimate of the surface-to-internal dose ratio.

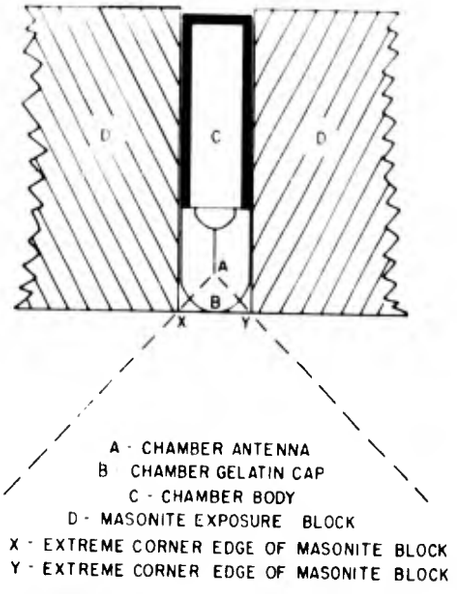

Figure 6.1 Cross section of ionization chamber in masonite block depicting restricted radiation geometry.

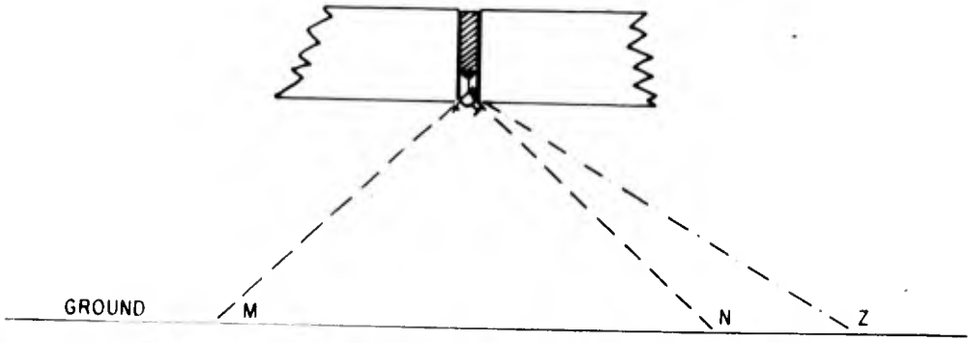

Figure 6.2 Typical exposure condition illustrating geometry deficiency.

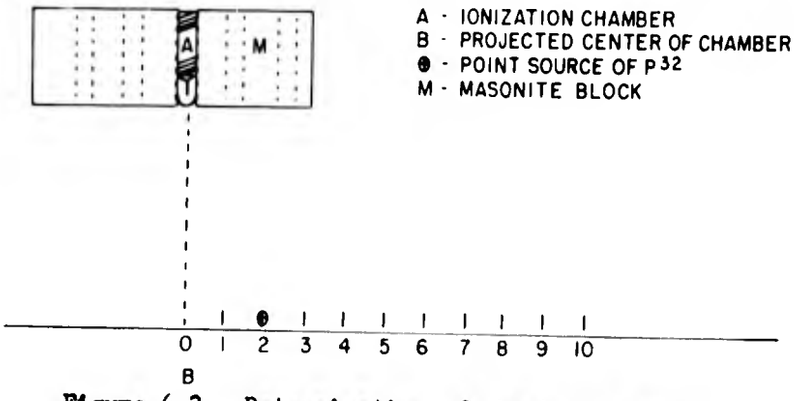

Figure 6.3 Determination of chamber geometry.

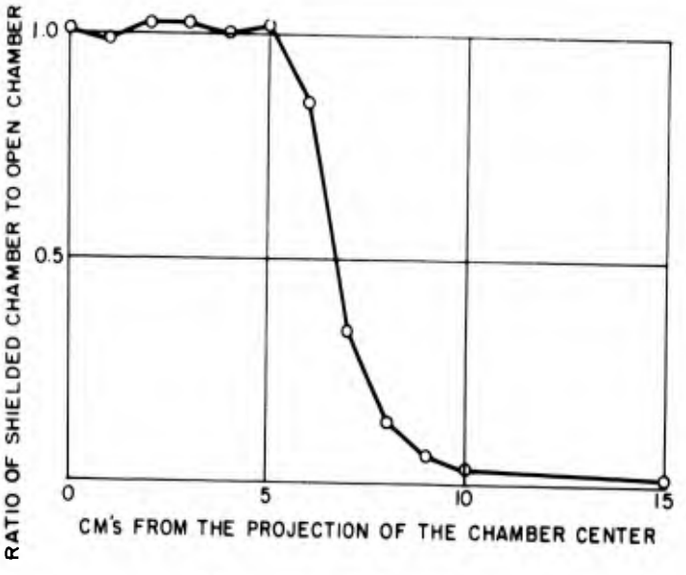

Figure 6.4 Ratio of restricted geometry to 2 -steradian geometry with respect to horizontal displacement of the source.

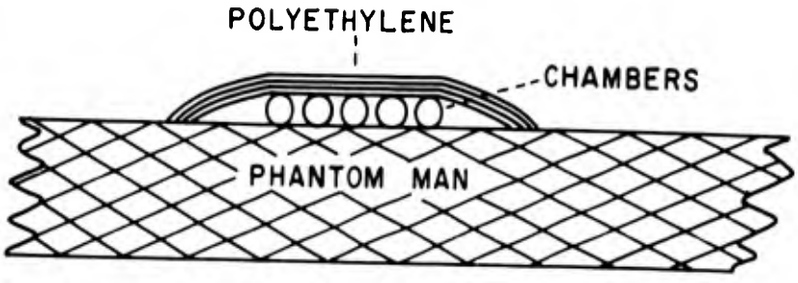

Figure 6.5 Absorption study with unrestricted geometry.

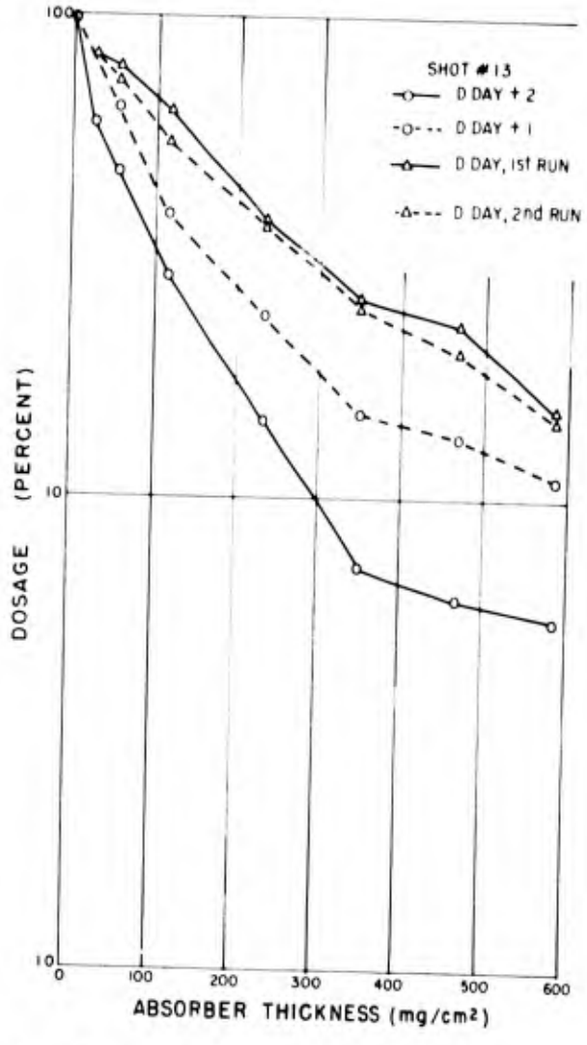

Figure 6.6 Absorption of radiation by polyethylene in unrestricted geometry.

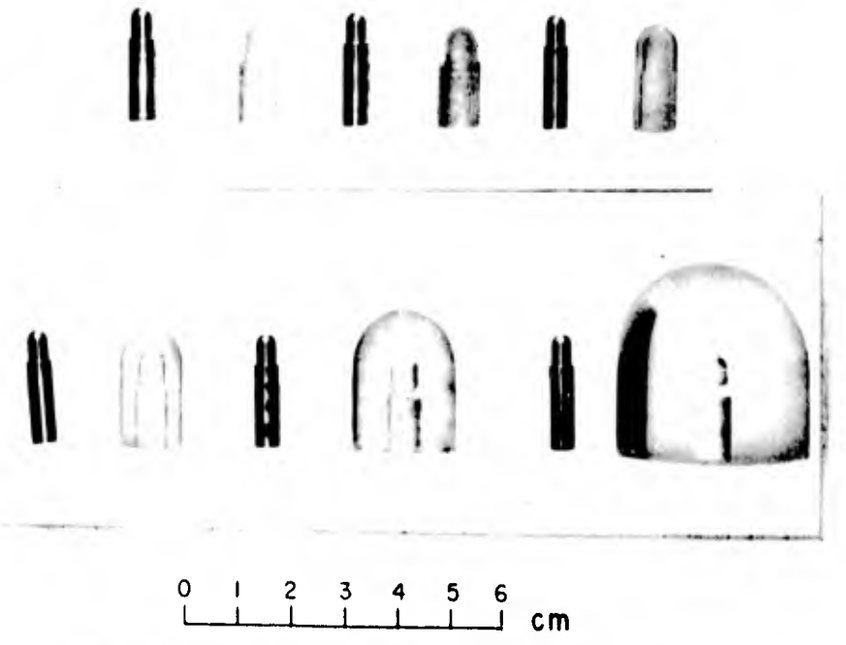

Figure 6.7 Lucite caps fitted to ionization chambers used in absorption studies.

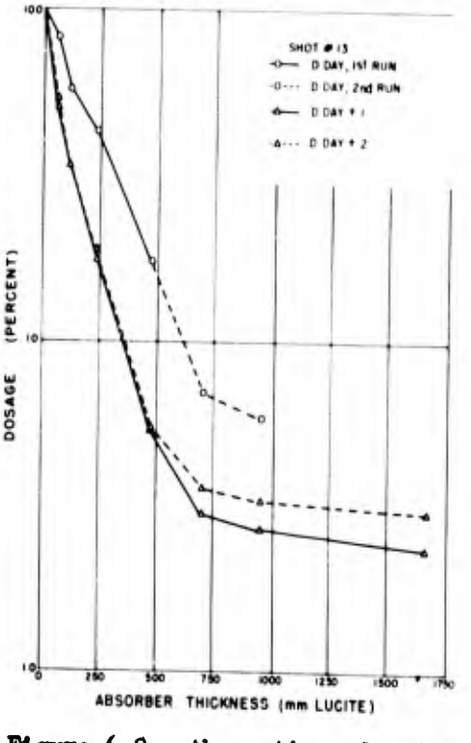

Figure 6.8 Absorption of radiation by lucite caps in unrestricted geometry.

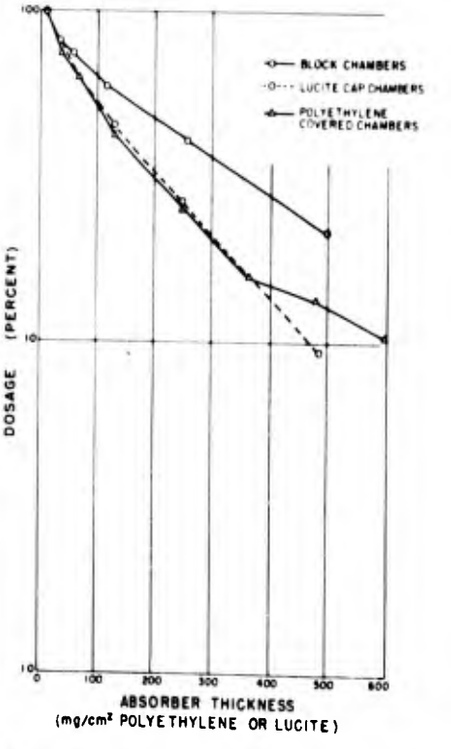

Figure 6.9 Comparison of the three geometrically different absorption systems using polyethylene.

CHAPTER 7

CONCLUSIONS AND RECOMMENDATIONS

7.1 CHARACTER OF THE RADIATION

7.1.1 Hard Component, Gamma. The absorption studies made with copper and gold indicate a moderately energetic gamma radiation. In no case did 3,000 mg/cm^2 of either copper or gold attenuate this hard component by more than 10 percent.

Dose determinations made at several different interior locations in the human phantom gave identical readings, irrespective of the depth within the body at which the determination was made. Only relatively energetic gamma radiation could give rise to such data.

7.1.2 Soft Component, Beta. One of the more important considerations of this work was the question of whether low-energy gamma radiation or high-energy beta particles were predominantly responsible for the high surface dose to a man in a fallout field. The data strongly suggest substantial quantities of beta radiation whose effective energy is quite similar to that of radioactive phosphorous, P^{32}, 1.7 Mev.

7.2 UPRIGHT MAN

A man standing upright in a radiation fallout field would receive a dose at internal points of the body, regardless of height above the ground, roughly equivalent to the reading of the average gamma reading survey meter. However, the surface dose at any part of the body is a function of distance from the ground and can be as much as an order of magnitude higher than the internal dose. Further, the geometry, or shape, of the body has little to do with either the surface or internal dose received at any point.

7.3 PRONE MAN

A man lying prone in a fallout field of radiation is subject to an intense ground-side surface dose in comparison to the internal dose received. This surface dose may be as high as 20 to 1 over the

internal dose during the first day after a nuclear explosion, and decreases thereafter as a function of time. The top surface of a prone man will receive approximately the same dose as the interior.

7.4 REMOVAL OF GROUND CONTAMINATION BY BRUSHING

Brushing of the ground, such as might be done by an infantryman with his arms, is quite effective in substantially lowering the front surface dose when he is in a prone position. Light brushing of the soil, if the soil is of such composition as to facilitate significant top soil removal, can be responsible for lowering the bottom surface dose by as much as 50 percent. However, brushing has little effect upon the internal dose and the top surface dose of the prone man, lowering these doses by less than 10 percent. Therefore, only a small fraction of the hard component, which is responsible for the dose to the internal organs and top surface of the prone man, is originating from that area that has actually been brushed. Also, the remaining bottom surface dose is primarily gamma radiation coming from areas other than that which was brushed.

7.5 VERTICAL GRADATION OF DOSE

Measurements of vertical gradation of dose show a factor of four differential between 5 and 180 cm. Any observed factor-relationship for a distance between two heights will be dependent upon so many variables that the data presented in Chapter 5 regarding this is little more than informative in nature. Only by measuring each particular situation for the data desired will vertical gradation of dose have meaning.

7.6 APPLICATION TO HUMAN HAZARD

A potential hazard may be presumed in the presence of any ionizing radiation; it is the penetrating power in tissue of these radiations which is the primary determining factor of the degree of hazard imposed. The surface doses observed, often 20 times higher than the gamma reading, may constitute a serious radiation dosage. The data presented here shows that this surface dose penetrates to the depths of known radiation-sensitive tissue. However, the relative hazard of the surface dose in relation to the internal dose of a man exposed to a residual radiation field is a difficult medical problem and cannot be evaluated here.

The specific ionizing strength of most beta radiation is approximately 50 to 100 times that of most gamma rays. However, beta radiation loses its energy by ionization rapidly in transversing tissue, rarely penetrating deeper than 10 mm from the surface. It becomes a point of conjecture as to which is the predominant mechanism affecting the hazard; the high specific ionization or the limited maximum range of beta particles. Each tends to compensate for the other.

It is not difficult to evaluate the tissue penetration of beta radiation from a fallout field, but the proper interpretation of the

degree of hazard imposed by the penetration is difficult. Each different degree of tissue penetration poses a distinct biological response problem in itself.

7.7 RECOMMENDATIONS

The project work has provided much necessary data regarding the character of the radiation and its penetrating power in several geometrical situations typical of fallout, in order that an investigation of the human hazard resulting from such radiation might be initiated. A collaborative and practical project should be initiated with the biological and physical scientists participating to evaluate the degree of human hazard prevailing in a fission-product fallout field that is not now being measured.

If such a project is undertaken, a new approach to instrument design is indicated. Inasmuch as a surface dose, per se, has little meaning without knowledge of the penetrating power of this radiation in tissue, little will be gained by a combination of "open-window" and "closed-window" readings. It appears that three distinct radiation readings taken on any source will be necessary to evaluate properly the human hazard. There should be a surface reading (open window), a gamma reading (closed window), and some intermediate absorber-thickness reading to evaluate the penetrating power of the surface dose. With these three readings a nomograph system to evaluate the human hazard could be utilized. Considering Figure 7.1 and Figure 7.2, if point A is a surface reading, point B some intermediate thickness, and point C a gamma-only reading, it is obvious that while the ratio of A/C will be identical for each of the two figures, the ratio of B/C will be different. Further, it is obvious that the theoretical dose originating from Figure 7.2 will be much more body damaging than the dose of radiation stemming from the field creating Figure 7.1, owing to the greater penetrating power of the soft component of Figure 7.2. The relationship between the ratios of A/C and B/C could be correlated to human hazard.

Although the work described here has been confined to fission fallout field, the above-mentioned instrument design should be applicable to all radiation measurements.

The results of this and other work suggest that there is little more to be gained from the future use of phantoms for such measurements. If, however, a biological evaluation of the degree of hazard caused by this usually unmeasured soft component indicates a serious situation, more extensive phantom measurements might be indicated for solving some specific problem, rather than the generalized type of study done in this work.

Figure 7.2 Comparison of penetrating power of two different fields.

Figure 7.1 Comparison of penetrating power of two different fields.

REFERENCES

1. Condit, R. I., J. P. Dyson, and W. S. S. Lamb; An Estimate of the Relative Hazard of Beta and Gamma Radiation from Fission Products, NRDL Report AD-95(H), April, 1949, UNCLASSIFIED.

2. Parker, H. M.; Recent Advances in Biological and Medical Physics, by J. Lawrence and J. S. Hamilton, UNCLASSIFIED.

3. Brennan, J. T.; Beta-Gamma Skin Hazard in the Postshot Contaminated Area, WT-746, December, 1953, CONFIDENTIAL-RESTRICTED DATA.

4. Cronkite, E. P., et al; J.A.M.A. 159, 430, 1955, UNCLASSIFIED.

5. Dahl, A. H.; Effective Energy of Residual Gamma Radiation, WT-814, January, 1954, CONFIDENTIAL-RESTRICTED DATA.

6. Tochilin, et al; Beta Ray and Gamma Ray Energy of Residual Contamination, WT-372, April, 1952, SECRET-RESTRICTED DATA.

7. Chambers, F. W., Jr.; Residual Ionizing Radiation Depth Dose Measurements in Unit Density Material, WT-336, March, 1955, CONFIDENTIAL-RESTRICTED DATA.

8. Morgan, K. Z.; Personal Communication.

9. White, G. R.; X-ray Attenuation Coefficients From 10 Kev and 100 Mev, National Bureau of Standards Report 1003, May, 1952, UNCLASSIFIED.

DISTRIBUTION

Military Distribution Categories 5-40 and 5-50

ARMY ACTIVITIES

1 Asst. Dep. Chief of Staff for Military Operations, D/A, Washington 25, D.C. ATTN: Asst. Executive (Rm 2E)

2 Chief of Research and Development, D/A, Washington 25, D.C. ATTN: Special Weapons and Air Defense Division

3 Chief of Ordnance, D/A, Washington 25, D.C. ATTN: ORDTX-AR

4- 6 Chief Signal Officer, D/A, R&D Division, Washington 25, D.C. ATTN: SIGRD

7- 8 The Surgeon General, D/A, Washington 25, D.C. ATTN: Chief, R&D Division

9- 10 Chief Chemical Officer, D/A, Washington 25, D.C.

11 The Quartermaster General, D/A, Washington 25, D.C. ATTN: Research and Development Div.

12- 16 Chief of Engineers, D/A, Washington 25, D.C. ATTN: ENGNB

17 Chief of Transportation, Military Planning and Intelligence Div., Washington 25, D.C.

18- 20 Commanding General, Continental Army Command, Ft. Monroe, Va.

21 President, Board #1, Headquarters, Continental Army Command, Ft. Sill, Okla.

22 President, Board #2, Headquarters, Continental Army Command, Ft. Knox, Ky.

23 President, Board #3, Headquarters, Continental Army Command, Ft. Benning, Ga.

24 President, Board #4, Headquarters, Continental Army Command, Ft. Bliss, Tex.

25 Commanding General, First Army, Governor's Island, New York 4, N.Y.

26 Commanding General, Second Army, Ft. George G. Meade, Md.

27 Commanding General, Third Army, Ft. McPherson, Ga. ATTN: ACofS, G-3

28 Commanding General, Fourth Army, Ft. Sam Houston, Tex. ATTN: G-3 Section

29 Commanding General, Fifth Army, 1660 E. Hyde Park Blvd., Chicago 15, Ill.

30 Commanding General, Sixth Army, Presidio of San Francisco, Calif. ATTN: AMGCT-4

31 Commanding General, U.S. Army Caribbean, Ft. Amador, C.Z. ATTN: Cml. Off.

32 Commanding General, USARPAC & MDW, Ft. Brooke, Puerto Rico

33 Commanding General, Southern European Task Force, APO 168, New York, N.Y. ATTN: ACofS, G-4

34- 35 Commander-in-Chief, Far East Command, APO 500, San Francisco, Calif. ATTN: ACofS, J-4

36 Commanding General, U.S. Army Forces Far East (Main), APO 343, San Francisco, Calif. ATTN: ACofS, G-4

37 Commanding General, U.S. Army Alaska, APO 942, Seattle, Wash.

38- 39 Commanding General, U.S. Army Europe, APO 403, New York, N.Y. ATTN: OCOT Div., Combat Dev. Br.

40-41 Commanding General, U.S. Army Pacific, APO 958, San Francisco, Calif. ATTN: Cml. Off.

42- 43 Commandant, Command and General Staff College, Ft. Leavenworth, Kan. ATTN: ALLIS(AC)

44 Commandant, The Artillery and Guided Missile School, Ft. Sill, Okla.

45 Secretary, The Antiaircraft Artillery and Guided Missile School, Ft. Bliss, Texas. ATTN: Mr. George D. Breitegam, Dept. of Tactics and Combined Arms

46 Commanding General, Army Medical Service School, Brooke Army Medical Center, Ft. Sam Houston, Tex.

47 Director, Special Weapons Development Office, Headquarters, CONARC, Ft. Bliss, Tex. ATTN: Capt. T. F. Skinner

48 Commandant, Walter Reed Army Institute of Research, Walter Reed Army Medical Center, Washington 25, D.C.

49 Superintendent, U.S. Military Academy, West Point, N.Y. ATTN: Prof. of Ordnance

50 Commandant, Chemical Corps School, Chemical Corps Training Command, Ft. McClellan, Ala.

51- 52 Commanding General, Research and Engineering Command, Army Chemical Center, Md. ATTN: Deputy for R&D and Non-Toxic Material

53- 54 Commanding General, Aberdeen Proving Ground, Md. (Under envelope) ATTN: RD Control Officer for Director, Ballistic Research Laboratory)

55- 56 Commanding General, The Quartermaster Center, Ft. Belvoir, Va. ATTN: Asst. Commandant, Engineer School

57 Commanding Officer, Engineer Research and Development Laboratories, Ft. Belvoir, Va. ATTN: Chief, Technical Intelligence Branch

58 Commanding Officer, Picatinny Arsenal, Dover, N.J. ATTN: [illegible]

59 Commanding Officer, Frankford Arsenal, Philadelphia 37, Pa. ATTN: Col. Lewis Kendel

60 Commanding Officer, Army Medical Research Laboratory, Ft. Knox, Ky.

61- 62 Commanding Officer, Chemical Corps Chemical and Radiological Laboratory, Army Chemical Center, Md. ATTN: Tech. Library

63 Commanding Officer, Transportation R&D Station, Ft. Eustis, Va.

64 Director, Technical Development Center, Picatinny Arsenal, Dover, N.J.

65 Director, Waterways Experiment Station, P.O. Box 631, Vicksburg, Miss. ATTN: Library

66 Director, Armed Forces Institute of Pathology, Walter Reed Army Medical Center, 6825 16th Street, N.W., Washington 12, D.C.

67 Director, Operations Research Office, Johns Hopkins University, 731 Connecticut Ave., Chevy Chase, Md. Washington 15, D.C.

68- 69 Commanding General, Quartermaster Research and Development Command, Quartermaster Research and Development Center, Natick, Mass. ATTN: CRD Liaison Officer

70 Commandant, The Army Aviation School, Fort Rucker, Alabama

71 President, Board No. 1, CONARC, Fort Rucker, Alabama

72- 73 Technical Information Service Extension, Oak Ridge, Tenn.

NAVY ACTIVITIES

74- 75 Chief of Naval Operations, D/N, Washington 25, D.C. ATTN: [illegible]

76 Chief of Naval Operations, D/N, Washington 25, D.C. ATTN: (OP-4)

77 Director of Naval Intelligence, D/N, Washington 25, D.C. ATTN: (OP-92)

78- 79 Chief, Bureau of Medicine and Surgery, D/N, Washington 25, D.C. ATTN: Special Weapons Defense Div.

80 Chief, Bureau of Ordnance, D/N, Washington 25, D.C.

81 Chief of Naval Personnel, D/N, Washington 25, D.C.

82- 83 Chief, Bureau of Ships, D/N, Washington 25, D.C. ATTN: Code [illegible]

84 Chief, Bureau of Yards and Docks, D/N, Washington 25, D.C. ATTN: D-440

85 Chief, Bureau of Supplies and Accounts, D/N, Washington 25, D.C.

86- 87 Chief, Bureau of Aeronautics, D/N, Washington 25, D.C.

88 Chief of Naval Research, Department of the Navy Washington 25, D.C. ATTN: Code 811

89 Commander-in-Chief, U.S. Pacific Fleet, Fleet Post Office, San Francisco, Calif.

90 Commander-in-Chief, U.S. Atlantic Fleet, U.S. Naval Base, Norfolk 11, Va.
97-100 Commandant, U.S. Marine Corps, Washington 25, D.C. ATTN: Code AO3H
101 President, U.S. Naval War College, Newport, R.I.
102 Superintendent, U.S. Naval Postgraduate School, Monterey, Calif.
103 Commanding Officer, U.S. Naval Schools Command, U.S. Naval Station, Treasure Island, San Francisco, Calif.
104 Commanding Officer, U.S. Fleet Training Center, Naval Base, Norfolk 11, Va. ATTN: Special Weapons School
105 Commanding Officer, U.S. Fleet Training Center, Naval Station, San Diego 36, Calif. ATTN: (SIWP School)
106 Commanding Officer, Air Development Squadron 5, VX-5, U.S. Naval Air Station, Moffett Field, Calif.
107 Commanding Officer, U.S. Naval Damage Control Training Center, Naval Base, Philadelphia 12, Pa. ATTN: ABC Defense Course
108 Commanding Officer, U.S. Naval Unit, Chemical Corps School, Army Chemical Training Center, Ft. McClellan, Ala.
109 Commander, U.S. Naval Ordnance Laboratory, Silver Spring 19, Md. ATTN: EH
110 Commander, U.S. Naval Ordnance Laboratory, Silver Spring 19, Md. ATTN: R
111 Commander, U.S. Naval Ordnance Test Station, Inyokern, China Lake, Calif.
112 Commanding Officer, U.S. Naval Medical Research Inst., National Naval Medical Center, Bethesda 14, Md.
113 Director, U.S. Naval Research Laboratory, Washington 25, D.C. ATTN: Mrs. Katherine H. Cass
114 Director, The Material Laboratory, New York Naval Shipyard, Brooklyn, N. Y.
115 Commanding Officer and Director, U.S. Navy Electronics Laboratory, San Diego 52, Calif.
116-119 Commanding Officer, U.S. Naval Radiological Defense Laboratory, San Francisco 24, Calif. ATTN: Technical Information Division
120 Commander, U.S. Naval Air Development Center, Johnsville, Pa.
121 Commanding Officer, Clothing Supply Office, Code 1D-0, 3rd Avenue and 29th St., Brooklyn, N.Y.
122 Commandant, U.S. Coast Guard, 1300 E. St. N.W., Washington 25, D.C. ATTN: Capt. J. R. Stewart
123-129 Technical Information Service Extension, Oak Ridge, Tenn. (Surplus)

AIR FORCE ACTIVITIES

130 Asst. for Atomic Energy, Headquarters, USAF, Washington 25, D.C. ATTN: DCS/O
131 Director of Operations, Headquarters, USAF, Washington 25, D.C. ATTN: Operations Analysis
132 Director of Plans, Headquarters, USAF, Washington 25, D.C. ATTN: War Plans Div.
133 Director of Research and Development, Headquarters, USAF, Washington 25, D.C. ATTN: Combat Components Div.
134-135 Director of Intelligence, Headquarters, USAF, Washington 25, D.C. ATTN: AFOIN-IB
136 The Surgeon General, Headquarters, USAF, Washington 25, D.C. ATTN: Bio. Def. Br., Pre. Med. Div.
137 Deputy Chief of Staff, Intelligence, Headquarters, U.S. Air Forces Europe, APO 633, New York, N.Y. ATTN: Directorate of Air Targets
138 Commander, 497th Reconnaissance Technical Squadron (Augmented), APO 633, New York, N.Y.
139 Commander, Far East Air Forces, APO 925, San Francisco, Calif.
140 Commander-in-Chief, Strategic Air Command, Offutt Air Force Base, Omaha, Nebraska. ATTN: Special Weapons Branch, Inspector Div., Inspector General
141 Commander, Tactical Air Command, Langley AFB, Va. ATTN: Documents Security Branch
142 Commander, Air Defense Command, Ent AFB, Colo.
143-144 Research Directorate, Headquarters, Air Force Special Weapons Center, Kirtland Air Force Base, New Mexico, ATTN: Blast Effects Research
145 Commander, Air Research and Development Command, Box 1395, Baltimore, Md. ATTN: RDDN
146 Commander, Air Proving Ground Command, Eglin AFB, ATTN: Adj./Tech. Report Branch
147-148 Director, Air University Library, Maxwell AFB
149-156 Commander, Flying Training Air Force, Waco, Tex. ATTN: Director of Observer Training
157 Commander, Crew Training Air Force, Randolph AFB, Tex. ATTN: 2CTS, DCS/O
158-159 Commandant, Air Force School of Aviation Medicine, Randolph AFB, Tex.
160-161 Commander, Wright Air Development Center, Patterson AFB, Dayton, O. ATTN:
162-163 Commander, Air Force Cambridge Research Center, Hanscom Field, Bedford, Mass.
164-166 Commander, Air Force Special Weapons Center, Kirtland AFB, N. Mex. ATTN: Library
167-168 Commander, Lowry AFB, Denver, Colo. ATTN: Director of Armament Training
169 Commander, 1009th Special Weapons Squadron, Headquarters, USAF, Washington
170-171 The RAND Corporation, 1700 Main St., Santa Monica, Calif. ATTN: Nuclear Energy
172 Commander, Second Air Force, Barksdale AFB, La. ATTN: Operations Analysis
173 Commander, Eighth Air Force, Operations Analysis Office
174 Commander, Fifteenth Air Force, March AFB, Calif. ATTN: Operations Analysis
175 Commander, Western Development Division, Inglewood, Calif. ATTN:
176-182 Technical Information Service Extension, Oak Ridge, Tenn. (Surplus)

OTHER DEPARTMENT OF DEFENSE ACTIVITIES

183 Asst. Secretary of Defense, Research and Development, D/D, Washington 25, D.C. ATTN:
184 U.S. Documents Officer, Office of the Military Representative, SHAPE, APO 55, N.Y.
185 Director, Weapons Systems Evaluation Group, WSEG No. 6, Pentagon, Washington 25, D.C.
186 Commandant, Armed Forces Staff College, Norfolk 11, Va. ATTN: Secretary
187-192 Commanding General, Field Command, Armed Forces Special Weapons Project, P.O. Box 5100, Albuquerque, New Mex.
193-194 Commanding General, Field Command, Armed Forces Special Weapons Project, P.O. Box 5100, Albuquerque, New Mex. ATTN: Technical Library
195-199 Chief, Armed Forces Special Weapons Project, Washington 25, D.C. ATTN: Documents Library Branch
200 Commanding General, Military District of Washington, Room 1E 868, Building T-7, Gravelly Point, Va.
201 Office of the Technical Director, Directorate of Effects Tests, Field Command, AFSWP, P.O. Box 57, Menlo Park, Calif. ATTN: Dr. F. B. Bull
202-207 Technical Information Service Extension, Oak Ridge (Surplus)

ATOMIC ENERGY COMMISSION ACTIVITIES

208-210 U.S. Atomic Energy Commission, Classified Technical Library, 1901 Constitution Ave., Washington 25, D.C. ATTN: Mrs. J. M. O'Leary (For DMA)
211-213 Los Alamos Scientific Laboratory, Report Library, P.O. Box 1663, Los Alamos, N. Mex. ATTN: Helen Redman
214-218 Sandia Corporation, Classified Document Division, Sandia Base, Albuquerque, N. Mex. ATTN: Martin J.
219-221 University of California Radiation Laboratory, P.O. Box 808, Livermore, Calif. ATTN: Margaret Falkenthal
222 Weapon Data Section, Technical Information Service Extension, Oak Ridge, Tenn.
223-265 Technical Information Service Extension, Oak Ridge (Surplus)